

Habitat Distribution Change of Commercial Species in the Adriatic Sea during the COVID-19 Pandemic

Gianpaolo Coro^{a,1,2,*}, Pasquale Bove^a, Anton Ellenbroek^b

^a*Istituto di Scienza e Tecnologie dell'Informazione "Alessandro Faedo" – CNR, Pisa, Italy*

^b*Food and Agriculture Organization of the United Nations, Viale delle Terme di Caracalla, 00153 Rome, Italy*

Abstract

The COVID-19 pandemic has led to reduced anthropogenic pressure on ecosystems in several world areas, but resulting ecosystem responses in these areas have not been investigated. This paper presents an approach to make quick assessments of potential habitat changes in 2020 of eight marine species of commercial importance in the Adriatic Sea. Measurements from floating probes are interpolated through an advection-equation based model. The resulting distributions are then combined with species observations through an ecological niche model to estimate habitat distributions in the past years (2015-2018) at 0.1° spatial resolution. Habitat patterns over 2019 and 2020 are then extracted and explained in terms of specific environmental parameter changes. These changes are finally assessed for their potential dependency on climate change patterns and anthropogenic pressure change due to the pandemic. Our results demonstrate that the combined effect of climate change and the pandemic could have heterogeneous effects on habitat distributions: three species (*Squilla mantis*, *Engraulis encrasicolus*, and *Solea solea*) did not show significant niche distribution change; habitat suitability positively changed for *Sepia officinalis*, but negatively for *Parapenaeus longirostris*, due to increased temperature and

*Corresponding author

Email addresses: coro@isti.cnr.it (Gianpaolo Coro), pasquale.bove@isti.cnr.it (Pasquale Bove), anton.ellenbroek@fao.org (Anton Ellenbroek)

¹Telephone Number: +39 050 315 8210

²Fax Number: +39 050 621 3464

decreasing dissolved oxygen (in the Adriatic) generally correlated with climate change; the combination of these trends with an average decrease in chlorophyll, probably due to the pandemic, extended the habitat distributions of *Merluccius merluccius* and *Mullus barbatus* but reduced *Sardina pilchardus* distribution. Although our results are based on approximated data and reliable at a macroscopic level, we present a very early insight of modifications that will possibly be observed years after the end of the pandemic when complete data will be available. Our approach is entirely based on Findable, Accessible, Interoperable, and Reusable (FAIR) data and is general enough to be used for other species and areas.

Keywords: Ecological Niche Modelling, Marine Science, COVID-19, Conservation biology

1. Introduction

The COVID-19 pandemic has directly affected human activities in many world areas (Coro and Bove, 2022), but its direct and indirect effects on the ecosystems of these areas are still under study. The reduced anthropogenic pressure on these ecosystems may have been beneficial for species habitats. However, the combined effects of the pandemic and climate change may have triggered complex reactions. Analysing natural pattern changes can reveal how ecosystems have responded to general climatic trends and inter-annual climatic variations within the context of human pressure reduction in 2020. In particular, marine ecosystems, especially in the Adriatic Sea, have benefited from the reduction of stress factors such as (i) fishing and vessel traffic (Depellegrin et al., 2020), (ii) disturbance of species life (Kemp et al., 2020), (iii) nutrient load in coastal areas (Adwibowo, 2020; Mishra et al., 2020; Shehhi and Samad, 2021), and (iv) water pollution (Yunus et al.,

22 2020). Understanding these benefits is interesting to quantitatively assess the peculiar ma-
23 rine ecosystem dynamics modifications that occurred at various levels (e.g., pollution,
24 biodiversity, and ecosystems) and how these influenced human activities (e.g., fisheries,
25 ecosystem services, social interaction and mobility, and illegal activities) (Snapshot-CNR,
26 2020). Understanding these dynamics allows identifying correlations that would have
27 been hidden without the lockdowns and help designing novel strategies for marine re-
28 source sustainability. For example, the lockdowns have allowed scientists to better model
29 the resilience of Adriatic fishing fleets to activity closure, i.e., the time to return to regime
30 fishing activity and market saturation (Coro et al., 2022). Moreover, the 2020 lockdown
31 restrictions to fishing activities in many areas (including the Adriatic) have limited scien-
32 tific survey ranges and resulted in missing survey hauls with consequent information loss
33 on stock biomass in 2020. This scenario calls for solutions to estimate biomass variation in
34 2020 despite the data gaps, which in turn requires information about habitat modification
35 as support to expert observations, biomass estimates, and fishing catch change understand-
36 ing (Brown et al., 2010; Weatherdon et al., 2016; Trifonova et al., 2017; Coro et al., 2020,
37 2021).

38 This paper analyses the potential habitat change, in 2020, of eight marine species
39 of commercial importance in the Adriatic Sea: European hake (*Merluccius merluccius*),
40 common sole (*Solea solea*), mantis shrimp (*Squilla mantis*), red mullet (*Mullus barba-*
41 *tus*), common cuttlefish (*Sepia officinalis*), European anchovy (*Engraulis encrasicolus*),
42 European pilchard (*Sardina pilchardus*), and deep-water rose shrimp (*Parapenaeus lon-*
43 *girostris*). These species are target of beam (common sole, mantis shrimp, common cut-
44 ttlefish), bottom (red mullet, deep-water rose shrimp, European hake), and mid-water (Eu-

ropean anchovy and pilchard) trawlers and purse seine vessels (European anchovy and pilchard). They currently account for about 70% of the total catch in the basin (FAO, 2020). The related fishing grounds range from coastal and offshore waters to deeper waters (e.g., the Pomo Pit) (Russo et al., 2020). The high fishing stress on these species and most Adriatic stocks (Froese et al., 2018) makes them relevant to understand how the combination of reduced anthropogenic stress during the COVID-19 pandemic and climatic changes influenced their distribution in the Adriatic. The study presented in this paper sheds light on the magnitude of change in one year of reduced anthropogenic pressure. Additionally, it indicates the sensitivity of the species' habitats to environmental change and can be used to predict the economic and ecological impact of a return to the pre-pandemic human activity level.

Habitat assessment often estimates the *ecological niche* of a species (Jones et al., 2012; Coro et al., 2016a; Weber et al., 2017; Deneu et al., 2021), i.e., the set of resources and environmental conditions that foster its persistence and proliferation in an area. It indicates such conditions either in the species' native habitat (native niche) or in other geographical areas (potential niche). Mathematically, a species' ecological niche is the space within a hyper-volume, in a vector space made up of environmental parameters, associated to the species' proliferation. Ecological niche models (ENMs) both estimate the parameters to use in the vector space and identify the hyper-volume boundaries. As a first step, an ENM uses statistical analysis or machine learning to estimate a predictive function between species observation records and specific environmental parameters. As a second step (projection phase), it applies the predictive function to other environmental parameter values that refer to a new area or other environmental scenarios (Peterson et al., 2007).

68 For example, a model trained on the environmental parameters of an area in 2015 can
69 be projected onto the parameter values in 2020 (Coro et al., 2018c; Coro, 2020). In the
70 experiment presented in this paper, individual ENMs for the eight selected species were
71 estimated for average environmental parameter values of the 2015-2018 years. Then they
72 were projected onto the environmental parameters of 2020 to see if the COVID-19 re-
73 lated changes influenced habitat distribution change. Furthermore, the major parameters
74 driving change were checked against other studies to assess if the observed variations po-
75 tentially depended on climate change (rather than inter-annual climatic variations) or the
76 pandemic. Our experiment was conducted in a context of minimal environmental and
77 species-occurrence data available for the pandemic period. Information extraction tech-
78 niques were therefore used to estimate enough information to feed the ENMs. Pattern
79 recognition was finally used to infer habitat change information over the years.

80 ENMs have been used to identify suitable areas for species (Peterson, 2003; Menchetti
81 et al., 2019). The generality of the approach made them adopted in early predictions of the
82 potential spread of COVID-19 due to environmental and meteorological conditions, e.g.,
83 they foresaw the lower summer outbreak rate of 2020 (Araujo and Naimi, 2020; Coro,
84 2020). These models have demonstrated a sufficient prediction effectiveness when work-
85 ing with few data, for example to predict rare species distributions (de Siqueira et al., 2009;
86 Coro et al., 2013a, 2015b; Chunco et al., 2013). The possibility to process environmental
87 parameters over time also makes them effective to monitor long-term habitat change (Ben
88 Rais Lasram et al., 2010; Friedlaender et al., 2011; Ashraf et al., 2017; Coro et al., 2016a,
89 2018c; Chala et al., 2019). ENMs commonly require uniformly distributed environmental
90 parameters estimated from real observations over the study area. These distributions can

91 result from hydrodynamic models based on point observations coming from satellite (Du-
92 rand et al., 2010; Werdell and Bailey, 2005; Alvera-Azcárate et al., 2005) or *in situ* probes
93 (Peterson, 2001; Huang et al., 2008; Ravdas et al., 2018; Scarponi et al., 2018). Effective
94 distributions are also obtainable through lower-complexity models, based on the advec-
95 tion equation that simulates the dispersion of a quantity by currents (Lipizer et al., 2014;
96 Troupin et al., 2012; Djakovac et al., 2015). Parameters estimated from these models com-
97 monly find applications in ecological models (Toonen and Bush, 2020; Garcia et al., 2019;
98 Blackford, 2002) and ecological niche models (Coll et al., 2007; Azzolin et al., 2020).
99 Accurate parameter selection is also integral to ENMs, because these models are sensitive
100 to mutually-dependent variables and achieve higher performance when using independent
101 variables (Pearson, 2007). A correct variable selection is typically achieved through sta-
102 tistical analysis (Sánchez-Tapia et al., 2017; Guo and Liu, 2010; Muscarella et al., 2014;
103 Magliozzi et al., 2019; Schnase et al., 2021) or other ENMs (Warren and Seifert, 2011;
104 Coro et al., 2013a, 2015b,a; Zeng et al., 2016; Bargain et al., 2017).

105 This paper proposes a workflow based on the application of ENMs to *in situ* environ-
106 mental parameter observations and expert-verified species observations to discover habitat
107 change across 2015-2018, 2019, and 2020. The 2015-2018 period was used as an aggre-
108 gated and meaningful reference for average environmental conditions and species presence
109 in the near past, and 2019 data were used to assess if the variations observed in 2020 were
110 due to the pandemic or climate change. First, punctual environmental observations were
111 transformed into uniform parameter distributions through an advection equation-based
112 model. Second, parameter selection per species was conducted to feed ENMs with the
113 parameters mostly associable with the species habitat (e.g., its preferred depth range and

114 environmental conditions). Third, the consistency of our ENMs was verified against other
115 ENMs calculated independently. Fourth, habitat variation over the years, per species, was
116 studied to identify habitat change trends. Finally, these trends were explained in terms of
117 environmental parameter change potentially correlated with climate change and the pan-
118 demic. Our study used only a few, but reliable, environmental and species data. This
119 choice was made to investigate the viability of open data and thus to only use actual obser-
120 vations whose modulations contained information on the reduced anthropogenic pressure
121 in 2020 due to the pandemic.

122 Our analysis identified robust patterns at the Adriatic scale but cannot be considered
123 punctually reliable because it is based on few data (i.e., it is a data-poor approach). Nev-
124 ertheless, it offers an unprecedented possibility to shed light on the modifications that the
125 combined action of the COVID-19 pandemic and climate change brought to species' dis-
126 tribution in the Adriatic Sea, way ahead of the time when data will be collected, collated,
127 and analysed after the end of the pandemic. The open data approach was possible thanks
128 to the recent investments by international communities on Findable, Accessible, Interop-
129 erable, and Reusable (FAIR) data, Open Science, and data collection networks addressing
130 the realisation of digital twins of marine systems (EU Commission, 2020b).

131 **2. Methods**

132 *2.1. Data*

133 Our experiment used the data of the international Argo float network (Argo, 2000).
134 This network includes robotic probes that drift with ocean currents while moving and
135 measuring biogeochemical parameters along the water column. These probes collect en-

136 vironmental information with sampling frequencies ranging from 2s to several minutes,
137 reaching down to 2000 m in 10-day data collection cycles. Data streams are transmitted
138 via satellite to distributed information centres (Global Data Assembly Centers, GDACs).
139 GDACs make the data freely available for download (Argo, 2000). Argo currently ex-
140 poses over 20-years of data and manages ~4000 operational floats. Floats are located
141 worldwide except for ice zones, with a higher density in the equatorial belt. The collected
142 environmental parameters include depth, pressure, dissolved oxygen, ocean-current speed
143 components, practical salinity, temperature, wind-stress components, electrical conductiv-
144 ity, chlorophyll-a, and fluorescence. Argo data can be included in the class of FAIR data as
145 being free, timely, and unrestricted-access data (Tanhua et al., 2019). Data access has the
146 only policy to acknowledge the Argo network in scientific publications. Ethical oversight
147 is left to the individual scientists or organizations using the data.

148 To use Argo data in our niche models, they were aggregated and processed to reduce
149 noise and computational complexity. Three groups of data were selected and downloaded
150 from the GDACs - in CSV format - for the Adriatic Sea (using a bounding box extension of
151 [+8;+20] longitude and [+38;+46] latitude). The first dataset contained observations from
152 2015 to 2018; the second included observations collected in 2019; the third contained
153 observations collected in 2020. The 2015-2018 range represents an aggregated reference
154 of environmental conditions in the near past. This aggregation was necessary to provide
155 reference statistical averages for the environmental parameters and allowed collecting a
156 meaningful set of species observations for training ENMs. The 2019 data were used as a
157 reference to assess if the variations observed in 2020 were either due to the pandemic or
158 continuing trends from the previous years (possibly related to climate change). The 2020

159 data were assumed to contain observations with signals of the COVID-19 pandemic and
160 climate change.

161 Argo data were averaged at a 0.1° resolution to increase statistical viability (Coro et al.,
162 2018b). The following parameters were extracted from the CSV data: temperature ($^\circ\text{C}$),
163 salinity (PSU), chlorophyll-a (mg/m^3), dissolved oxygen (DOX) ($\mu\text{mol}/\text{kg}$). These are
164 indeed the most abundant and reliable data downloadable from Argo. For each parameter,
165 average values were calculated for surface range, seafloor (bottom), and the entire water
166 column. Surface and bottom ranges were identified as the first and last ranges of a log-
167 arithmic division, into five parts, of the maximum depth of each 0.1° cell in the Adriatic
168 (Reyes, 2015; Coro et al., 2018b). Instead of using static ranges, this approach adapted
169 the definition of surface and bottom ranges to the specific cell depth. It normally results
170 in better niche modelling, especially for benthic and demersal species (Ready et al., 2010;
171 Reyes, 2015). For each parameter, surface, bottom, and average (in the water column) val-
172 ues were estimates at 0.1° resolution. Furthermore, locations outside of the Adriatic Sea
173 were excluded by only using those within the geographical subareas 17 and 18 of the Gen-
174 eral Fisheries Commission for the Mediterranean (GFCM, 2020). This process generated
175 36 datasets overall, as the results of three aggregation types (surface, bottom, average), for
176 each aggregation time (2015-2018, 2019, 2020), repeated for four parameters.

177 As a final step, consistency between the observations from the different datasets was
178 enhanced by constraining all datasets to cover the same areas. Different spatial coverage
179 over the years can indeed be a source of bias. For example, if observations covered north
180 Adriatic more extensively than south Adriatic in a particular year, sampling would be
181 northward skewed with consequent over-representation of northern environmental values.

182 If this is not the case for the other years, inconsistency between parameter sampling and
183 representation will occur. To avoid this issue, only probes locations that were present in all
184 reference years were retained. A 0.5° spatial tolerance was used in the selection of these
185 locations.

186 The ENM used in the present experiment required environmental data uniformly dis-
187 tributed over the Adriatic Sea. Consequently, all 0.1° cells required an environmental value
188 assigned, either averaged from the Argo observations or estimated through a model. Given
189 the low density and quantity of the available environmental observations (Section 3) and
190 the importance of currents in the biogeochemical components' drift and spread in the Adri-
191 atic, parameter values were interpolated through a model based on the advection equation
192 and depth information. In particular, the Data-Interpolating Variational Analysis (DIVA)
193 was used (Barth et al., 2010). DIVA is commonly used to produce uniform distributions of
194 environmental parameters (Coro et al., 2018a; Coro and Trumphy, 2020; Schaap and Lowry,
195 2010) and solves the advection equation to simulate the transport of a substance or quantity
196 by currents. DIVA also estimates the mutual spatial correlation between observations and
197 requires minimal parametrisation to produce high-quality interpolation at a user-defined
198 resolution (Troupin et al., 2010, 2012; Coro et al., 2016c). Internally, DIVA reconstructs
199 a continuous field from discrete measurements through a numerical implementation of the
200 Variational Inverse Model (Bennett, 1992). This algorithm fits a continuous field to the
201 data through a minimization cost function (Watelet et al., 2016), using a finite-element
202 statistical method that embeds topographic and dynamic constraints (based on bathymetry
203 and oceanic-currents data). It can process irregularly-spaced observations to produce esti-
204 mates on a regular grid. Based on this fit, DIVA estimates a triangular-element mesh over

the interpolation area, where the characteristic length of each element is directly linked to the mutual spatial correlation between observations.

For our experiment, DIVA was applied to all Argo-aggregated data described in Section 2.1. Data of ocean current components were taken as NetCDF files from the Global Ocean Physic Analysis dataset hosted by the Copernicus Marine Service (Von Schuckmann et al., 2018). In addition, depth information was taken from the GEBCO-2020 bathymetry dataset, a global terrain model for ocean and land with 0.0042° uniform spatial resolution (GEBCO, 2020). To execute DIVA, the D4Science e-Infrastructure computational platform was used (Candela et al., 2016; Coro et al., 2015a, 2017; Assante et al., 2019). As a result, 36 uniform parameter distributions at 0.1° resolution for our environmental parameter aggregations were produced and represented with the ESRI-grid format (ASC).

2.2. *Species observations*

In order to extract species observation data, we consulted the Ocean Biogeographic Information System (OBIS) (Grassle, 2000). OBIS contains taxonomic and occurrence information for ~155,000 marine species and provides access to more than 163 million observation records, integrated from more than 4,000 sources. Its contributors include international research projects, national monitoring programs, museums, and individuals. OBIS is suitable for data mining and pattern recognition experiments, especially in data-poor scenarios where the quality of the data is fundamental to produce reliable analyses (Coro et al., 2013b, 2015c, 2016b, 2018c). The OBIS data quality checking is integral to ecological niche models that are particularly sensitive to data bias (Coro et al., 2015b). Furthermore, for each occurrence record, OBIS indicates if it underwent expert verifica-

tion. This feature makes OBIS more suited for ecological niche modelling in data-poor scenarios than other data collections (Coro et al., 2015b,c). In our experiment, the OBIS observation records in the Adriatic Sea, between 2015 and 2018, that underwent expert verification were retrieved for the eight species under study. Their coordinates were stored as CSV files to feed ENMs later.

2.3. Ecological Niche Modelling

Maximum Entropy (MaxEnt) is a widely used ENM for marine species (Raybaud et al., 2015; Angeletti et al., 2020; Capezzuto et al., 2018). MaxEnt is a shallow machine learning model that estimates a function $\pi(\bar{x})$ defined over real-valued vectors \bar{x} of environmental parameters. This function is forced to reach maxima on the parameters associated with a species' presence and minima on absence-related parameters. Following a common abuse of notation, $\pi(\bar{x})$ can be considered a proxy of a probability density of a species' presence given the \bar{x} environmental parameters (Phillips and Dudík, 2008; Elith et al., 2011; Merow et al., 2013). MaxEnt learns the relation between environmental values in the species-observation locations and the general species' presence (Pearson, 2007; Coro et al., 2018c). One advantage of this model is that it can work with species-presence information only, but it is over-sensitive to biased data (Elith and Graham, 2009; Coro et al., 2015b). A MaxEnt model trained with parameters and species observations at 0.1° resolution will produce a probability distribution of species presence over the 0.1° cell subdivision of a study area. The $\pi(\bar{x})$ function is thus the probability that a 0.1° cell is suitable species habitat. MaxEnt estimates $\pi(\bar{x})$ after maximising the entropy function $H = -\sum \pi(\bar{x}) \ln(\pi(\bar{x}))$ on the training locations with respect to randomly-selected environmental parameter vectors in the study area (*background points*). In the present

experiment, \bar{x} was made up of 13 parameters associated with the 2015-2018 year range: temperature, salinity, chlorophyll-a, DOX (with related surface, bottom, water-column aggregations), and depth (from the GEBCO-2020 bathymetry data set). Although depth was constant through the years, it was included in our models because it is a fundamental parameter to estimate the niches of the studied species correctly. Depth was used as a proxy to model species preference to different seabeds and water column heights. Thus, it enhanced prediction reliability by adding complementary and valuable information about the species habitat. On the other hand, it was not functional to the subsequent pattern analysis. Training locations were those associated with the OBIS observations between 2015 and 2018. The used MaxEnt implementation (Phillips et al., 2021) accepted environmental parameters in ASC-raster format and species observation data in CSV format.

The training algorithm estimates the coefficients of a linear combination of the environmental parameters. These coefficients represent the weight of each environmental parameter in the species' environmental preferences (*percent contribution*). MaxEnt also estimates the *permutation importance* of each parameter in the \bar{x} vector. The training process is based on the following function definitions: $f(\bar{x})$, the probability density over the background parameters; $f_1(\bar{x})$, the density on the training set; and pr , the prior distribution (*prevalence*) of the species (equal to 0.5 when no prior assumption is available, as in our case). Based on these functions, $\pi(\bar{x})$ is defined as

$$\pi(\bar{x}) = \frac{f_1(\bar{x}) \cdot pr}{f(\bar{x})}$$

In a maximum entropy condition, the optimal $f_1(\bar{x})$ is the closest function to $f(\bar{x})$, because there would be no difference without species observations. Additionally, $f_1(\bar{x})$

272 should have maxima on the parameter means in the training set locations. With these
 273 constraints, the model minimises the Kullback-Leibler distance between $f_1(\bar{x})$ and $f(\bar{x})$

$$d(f_1(\bar{x}), f(\bar{x})) = \sum_{\bar{x}} f_1(\bar{x}) \cdot \log_2 \left(\frac{f_1(\bar{x})}{f(\bar{x})} \right)$$

274 This minimisation is solved by Gibbs distribution functions in the form $f_1(\bar{x}) = f(\bar{x})e^{\eta(\bar{x})}$
 275 (Phillips et al., 2006a), with $\eta(\bar{x}) = \alpha + \beta h(\bar{x})$; α being a normalization constant that
 276 makes $f_1(\bar{x})$ sum to 1; h being an optional transformation of \bar{x} that simulates a com-
 277 plex relation between the environmental parameters; and β being the *percent contribution*
 278 coefficients. The minimisation of $\eta(\bar{x})$ - which requires solving a log-linear equation -
 279 consequently minimises $d(f_1(\bar{x}), f(\bar{x}))$. The used MaxEnt software automatically solves
 280 this minimisation problem. It also estimates percent parameter contribution through an
 281 iterative process that calculates and accumulates the percent performance gain provided
 282 by each parameter (Phillips et al., 2017).

283 MaxEnt is generally preferred over linear and logistic regression for species habitat
 284 distribution modelling. It is equivalent to a Poisson regression (a generalized linear model)
 285 that is naturally suited for modelling the probability of a number of events in a fixed space
 286 (such as species occurrences) (Renner and Warton, 2013). Once the model parameters
 287 have been estimated, the $\pi(\bar{x})$ function can be used to estimate probability distributions
 288 over new parameter values than those of the training set, e.g. the parameters of locations
 289 outside of the study area (to discover the potential species niche) or new environmental
 290 scenarios (to study niche change over time) (Elith and Graham, 2009; Phillips et al., 2017).

291 MaxEnt is sensitive to sampling bias associated with species-observation locations and
 292 can over-fit small datasets (Merow et al., 2013; Wang et al., 2018). Our selected occur-

293 rence datasets were indeed small, as only expert-verified records were selected. They
294 also had potentially biased distributions, as they belonged to OBIS-included surveys with
295 frequent and fixed paths (Coro et al., 2015c). One way to manage this issue is to select
296 background points far away from the presence locations (Hengl et al., 2009). However,
297 our analysed species are common and widely distributed in the Adriatic, with absence lo-
298 cations potentially dense in the presence areas. Therefore, it was not possible to focus
299 background point sampling on specific areas. Providing the model with precise absence
300 and background locations would also have required more presence data and precise envi-
301 ronmental parameter distributions. However, specific studies on MaxEnt parametrisation
302 (Zaniewski et al., 2002; Dudík et al., 2005; Phillips and Dudík, 2008; Phillips et al., 2017)
303 have indicated general strategies to reduce presence location sampling and over-fitting bi-
304 ases, which include (i) selecting background points to reflect the same sampling bias as
305 the presence locations, (ii) including presence points among background points, (iii) using
306 *hinge* features to model complex species response to the environmental parameters and
307 make model fitting more flexible. The MaxEnt software used for this experiment offers
308 options to use *hinge* features and include presence locations among background points if
309 these are associated with unique combinations of environmental parameters (Phillips et al.,
310 2021). These options were used to attenuate over-fitting and sampling bias issues as far as
311 possible.

312 In the present experiment, MaxEnt was trained with 2015-2018 Adriatic environmental
313 data and species occurrence records to produce an ecological niche reference for the near
314 past. Then it was projected onto the 2019 and 2020 environmental data to analyse prob-
315 ability distribution change due to the different environmental parameters of these years.

316 Since the β vector indicates the parameters that carry the highest quantity of informa-
317 tion to understand species habitat preferences (Coro et al., 2018c; Coro, 2020), it can be
318 used to remove poorly niche-correlated parameters from the \bar{x} vector. This operation opti-
319 mally selects the variables associated with the species habitat (Section 3.1). For example,
320 deep-water and benthic species will likely be modelled with bottom-averaged parameters,
321 whereas pelagic species habitat will likely be modelled with water-column or surface re-
322 lated parameters. Furthermore, reducing the number of input environmental parameters
323 decreases the inter-dependence between the variables and improves the model accuracy
324 (Coro et al., 2015b). In the present experiment, the MaxEnt models of the studied species
325 were first trained with all parameters and then re-trained using only those parameters hav-
326 ing a *percent contribution* within 95% from the maximum contribution.

327 In summary, MaxEnt ENMs were produced for the 8 Adriatic species through the fol-
328 lowing steps: (i) MaxEnt models were trained with 2015-2018 OBIS observations and
329 interpolated environmental data; (ii) after a first training phase, the parameters with the
330 95% highest *percent contributions* were retained (thus, different parameter sets were as-
331 sociated to the different species); (iii) the models were re-trained only with the retained
332 parameters; (iv) the models were projected onto the 2019 and 2020 environmental param-
333 eters. The produced models will be referred to as *floating sensor* (FS) based models -
334 i.e., FS 2015-2018, FS 2019, and FS 2020 - to distinguish them from the baseline models
335 used for evaluation. A total of 24 models was thus produced, i.e., three models for each
336 analysed species.

337 2.4. Evaluation and pattern recognition

338 The ENM distributions were used to discover driving factors of species habitat change
339 over the years. The first goal of our quality evaluation was to assess the consistency of the
340 produced maps. As our second goal, the principal environmental drivers of habitat suit-
341 ability change were checked against evidence from general climate change and COVID-19
342 pandemic related trends. The entire evaluation process was managed through four *evalua-*
343 *tion questions*:

344 **Question 1:** *Are the produced distributions consistent?*

345 This question was answered by verifying the similarity between our models and other
346 ENMs. This operation confirmed that our models consistently captured the species' envi-
347 ronmental preferences, although they were trained on scarce and scattered data and tested
348 on the same training set (Section 3.1). Indeed, the partial reliability of our MaxEnt model
349 was assessed using the training data, but this was insufficient to state they were consistent,
350 due to the few data at hand. Thus, we set two consistency boundaries for our model: one
351 similarity and one dissimilarity reference. We used the similarity reference to confirm that
352 the produced distributions agreed with an independent habitat distribution. Instead, we
353 used the dissimilarity reference to check for significant difference with respect to a known
354 improbable scenario based on unlikely environmental parameter distributions.

355 The AquaMaps distributions were used for these tasks (Kaschner et al., 2006). They
356 were downloaded (not re-calculated) from the AquaMaps website (AquaMaps, 2020).
357 AquaMaps is a presence-only ENM that incorporates scientific expert knowledge into
358 species habitat modelling to account for known limitations of species occurrence records
359 (Corsi et al., 2000; Ready et al., 2010). We used AquaMaps as a mechanistic model

360 to estimate species distributions independently of the data available in our experiment.
361 Moreover, AquaMaps uses a complementary approach with respect to machine-learning-
362 based approaches because it explicitly models the causality between species presence and
363 environmental parameters (Pearson, 2007; Baker et al., 2018). AquaMaps has comparable
364 accuracy to GAM- and GLM-based ecological niche models (Ready et al., 2010). It is
365 particularly effective for large areas (e.g., the size of the Adriatic Sea) and when expert
366 knowledge about the species is available at the global scale. Moreover, it is reliable for
367 extracting macro-patterns of climate change influence on species distributions (Coro et al.,
368 2016a).

369 The AquaMaps *native* algorithm estimates the species niche distribution in its known
370 habitat. It uses a multiplication of environmental parameter envelopes whose ranges are
371 either statistically estimated or defined by an expert. The environmental parameters inte-
372 grated with the model are 0.5° resolution distributions of depth, salinity, temperature, pri-
373 mary production, distance from land, and sea ice concentration. In the present experiment,
374 the AquaMaps *native* model based on 2019 annual environmental parameters (hereafter
375 referred as *AquaMaps 2019*) was used as a similarity reference for our models.

376 As a dissimilar reference model, the AquaMaps *native-2050* model was used (hereafter
377 referred as *AquaMaps 2050*). This model integrates environmental parameters estimated
378 under the Special Report on Emissions Scenario (SRES) A2 of the Intergovernmental Panel
379 on Climate Change (IPCC). This scenario describes a future world with independent, self-
380 reliant nations with a continuously increasing population. Economic and technological
381 development are assumed to increase non uniformly across the world countries. Of key
382 importance are average surface temperature and salinity that have increasing trends (with

383 localised decreases for salinity), whereas ice concentration decreases globally and wa-
384 ter level increases. Our models were checked to be significantly distant from AquaMaps
385 2050 because this model represents an unlikely scenario for all selected species today.
386 Using the AquaMaps 2050 distributions as unlikely scenarios was particularly consistent
387 for our studied species because their 2050 distributions were significantly different from
388 the AquaMaps *native* distributions (Section 3). The AquaMaps *native* models were down-
389 loaded from the AquaMaps website (AquaMaps, 2020; Scarponi et al., 2018), whereas a
390 NetCDF FAIR version of the AquaMaps 2050 model was used, whose consistency and va-
391 lidity was confirmed by other experiments (Coro et al., 2018a). GDAL and CDO software
392 (OSGeo, 2019) was used to downsample the models to 0.1° resolution, through first-order
393 conservative remapping (Schulzweida, 2020), in order to be able to compare them with
394 our models.

395 **Question 2:** *Can habitat patterns be identified in 2020 with respect to the previous*
396 *years?*

397 A map comparison procedure was used to answer this question (described in Coro
398 et al. (2014)). This process calculates discrepancy and agreement between two maps. It
399 allows setting a threshold over each probability distribution to conduct presence/absence
400 comparison. Absences are values under the threshold and presences are values over the
401 threshold. The process then uses this classification to calculate discrepancy as the percent-
402 age cells where the two distributions disagree. It also calculates Cohen's kappa (Cohen
403 et al., 1960) to estimate agreement with respect to chance. Kappa is classified as poor,
404 slight, fair, moderate, substantial, or excellent according to the Landis and Koch range
405 classifications (Landis and Koch, 1977).

406 The three FS distributions of each species had different probability ranges. This issue
407 made it difficult to find a common threshold to compare low and high probability cells,
408 which is a common problem when comparing different distributions (Coro et al., 2014;
409 Phillips et al., 2006b). MaxEnt suggested potential habitat suitability thresholds out of a
410 training session over the 2015-2018 data, using a sensitivity-specificity analysis that con-
411 sidered only the observations and environmental data in 2015-2018. However, after this
412 training session, the MaxEnt model was projected onto the 2019 and 2020 data without
413 re-training, and this operation normally produces distributions with new probability ranges
414 (Phillips et al., 2006b; Coro and Bove, 2022). One approach to accommodate for this is-
415 sue is to allow MaxEnt to extend estimates beyond the parameter ranges observed on the
416 training set (i.e., to disable the model's *clamping* option). However, this technique should
417 be used with caution because it could generate inconsistent results or unnatural projec-
418 tions (Elith et al., 2011). Moreover, the approach assumes that the projection conditions
419 represent a completely different environmental scenario (e.g., in the far past or future). In
420 contrast, our projection scenarios fell within the *clamped* ranges for most variables (Sec-
421 tion 3.3). We also experimentally verified that clamping was not useful in overcoming this
422 issue with the data at hand.

423 Thus, the thresholds suggested by the sensitivity-specificity analysis over the 2015-
424 2018 data could not be used for the 2019 and 2020 distributions. Therefore, conducting a
425 fair comparison between the MaxEnt distributions required setting appropriate thresholds
426 for habitat suitability/unsuitability on each distribution separately; to transform a numer-
427 ical comparison into a consistent classification comparison. In this case, one possible
428 threshold to use is the first-quartile probability value, as also suggested by O'Brien (1980)

and Theil (1982). This property comes out of the observation that although the distribution ranges and shapes can differ between the models, one comparable measure of MaxEnt probability abundance (and thus of habitat suitability extent) is the number of elements with MaxEnt output value over the first quartile. Therefore, we used the first-quartile probability value of each FS distribution to identify areas of low and high suitability. Our results demonstrate that this approach generated comparable FS distributions (Section 3). As for AquaMaps, the log-linear nature of this model allows setting a 0.2 probability value as the threshold (Coro et al., 2013a, 2016a).

Since discrepancy and agreement calculation does not indicate if one distribution corresponds to more suitable habitat than the other, a new metric was introduced for this scope. In particular, a *suitability score* was defined on the discrepancy cells:

$$S = \frac{\sum_i P'_H(i) - \sum_i P''_H(i)}{N}$$

where i refers to cells on which the two dichotomic P' and P'' distributions differ; N is the total number of cells involved in the comparison; and $P'_H(i)$ and $P''_H(i)$ are the compared habitat distributions using new thresholds that identify *very high* probability zones. These thresholds were set to the 3rd quartiles of the FS distributions and to 0.8 for AquaMaps. The rationale behind the suitability score calculation is that if one distribution indicates very high suitability in the discrepancy areas more often than the other, that distribution is overall more favourable. Thus, $S > 0$ indicates that the first distribution is more suitable than the second (habitat *gain*) - and vice-versa when $S < 0$ (habitat *loss*) - whereas $S = 0$ indicates overall equal suitability between the two distributions (*stable* habitat).

450 Discrepancy, agreement, and suitability scores over the years can identify habitat change.
451 Increasing habitat suitability from 2015-2018 to 2019 and 2020 may indicate overall habi-
452 tat expansion (*gain*) in 2020, stable suitability may indicate unchanged habitat, and incon-
453 stant habitat gain and loss over the years can be associated with potential habitat change.

454 **Question 3:** *Which parameters drove habitat change in 2020?*

455 MaxEnt also produces single-parameter distributions by training the model with one
456 parameter at-a-time. These parameter distributions allow inferring the parameter ranges
457 that correspond to higher suitability. The inference is straightforward when the involved
458 parameters are independent or bring a high contribution (Coro et al., 2013a, 2015b, 2018c).
459 Our approach enhances parameter independence by re-training MaxEnt after removing
460 low-contributing parameters. Intersecting environmental parameter trends with MaxEnt
461 single-parameter distributions identifies the key responsible parameters for habitat change.

462 **Question 4:** *Do environmental parameter changes in 2020 depend on the COVID-19*
463 *pandemic or also on climate change?*

464 The change in key parameters for our selected species' habitat change could be due
465 to statistical inter-annual fluctuations, or to general global-scale changes such as climate
466 change or the reduction of anthropogenic pressure due to the COVID-19 pandemic. The
467 key factors were investigated by searching for other studies that specifically analysed these
468 parameters in other locations and correlated their trends to climate change or the pandemic.
469 This analysis, combined with the results from the previous evaluation phases, clarified the
470 correlation between anthropogenic pressure on ecosystems due to the COVID-19 pan-
471 demic, the coupling with climate change, and potential species habitat change.

472 2.5. Complete workflow

473 The complete workflow can be summarised as the production and comparison of Max-
474 Ent distributions of eight selected Adriatic Sea species out of OBIS species observations
475 and Argo data. Each step of the workflow has code and data associated in the open-source
476 repository linked to this paper (see Supplementary Material). The steps can be summarised
477 through the following *phases*:

478 **Phase 1:** Retrieve Argo data for the Adriatic and aggregate them at 0.1° spatial res-
479 olution (from <https://dataselection.euro-argo.eu/>). Select probes across
480 years that have a mutual distance under 0.5° . Produce surface, bottom, and water-column
481 average values for each environmental parameter in every reference time frame, i.e., 2015-
482 2018, 2019, and 2020. This phase generated 9 datasets (3 aggregations by 3 years) for
483 Argo parameters (4 in total), i.e., 36 datasets overall. All processing R code and results of
484 this phase are available in the repository linked in the Supplementary Material, within the
485 "Phase 1 - Argo Data Preparation" folder.

486 **Phase 2:** Interpolate the 36 environmental parameter datasets through DIVA, using
487 data on ocean current speed components and depth, to obtain uniform 0.1° distributions for
488 the entire Adriatic. Prepare the data as ASC files for MaxEnt. The used DIVA notebook
489 and the results of this phase are available in the repository linked in the Supplementary
490 Material, within the "Phase 2 - Environmental Parameter Distributions" folder.

491 **Phase 3:** Retrieve species occurrence records from OBIS ([https://obis.org/](https://obis.org/manual/access/)
492 [manual/access/](https://obis.org/manual/access/)) and prepare them for MaxEnt. For each species, use 2015-2018
493 OBIS species occurrence records and environmental datasets (plus depth from GEBCO)
494 within a MaxEnt model to produce 8 floating-sensor-based *full-variable* models for 2015-

2018 at 0.1° resolution. The retrieved and pre-processed OBIS occurrences, the data preparation scripts, the link to the MaxEnt software, and the MaxEnt results are available in the repository linked in the Supplementary Material, within the "Phase 3 - Occurrence Records and First MaxEnt Run" folder.

Phase 4: Execute MaxEnt again, for each species, using only the parameters that had the highest *percent contribution*, i.e., those within 95% relative difference from the maximum. This phase produced 8 final FS 2015-2018 models, one for each species. It also modelled each species with an optimal selection of parameters associated with their preferred depth ranges. For example, it selected depth and bottom-level parameters for deep-water and benthic species (Section 3.3). As a further step, project the MaxEnt models over the 2019 and 2020 parameter data to obtain FS 2019 and FS 2020 models for the 8 species. The MaxEnt re-execution results are available in the repository linked in the Supplementary Material, within the "Phase 4 - MaxEnt Re-application" folder.

Phase 5: Retrieve AquaMaps 2019 and 2050 distributions and downsample them to 0.1° for consistent comparison with the MaxEnt distributions. The retrieved AquaMaps distributions are available as ESRI-grid files in the repository linked in the Supplementary Material, within the "Phase 5 - AquaMaps Distributions" folder.

Phase 6: Extract parameter quantiles to study trends over the years. Compare MaxEnt distributions to quantify discrepancy and estimate habitat change (though suitability score). The results and the used scripts are available in the repository linked in the Supplementary Material, within the "Phase 6 - Estimate Quantiles" folder.

Phase 7: Identify patterns of habitat change (gain, loss, stability). The extracted patterns are available in the repository linked in the Supplementary Material, within the

518 "Phase 7 - Patterns" folder.

519 **Phase 8:** Study the main parameter trends to identify those that influenced habitat
520 change. Understand the relation between these trends and climate change and COVID-19
521 pandemic (Sections 3.3-3.4).

522 **3. Results**

523 Our method produced distribution maps for 2015-2018, 2019, and 2020 for each of
524 the eight analysed species (Figure 2). Referring to our evaluation questions (Section 2.4),
525 Section 3.1 addresses question 1; Section 3.2 addresses question 2; Section 3.3 addresses
526 question 3; and Section 3.4 addresses question 4.

527 For the present experiment, our workflow processed overall 2,166,025 *in situ* observa-
528 tions for 2015-2018, 364,219 observations for 2019, and 463,352 observations for 2020.
529 These observations covered from ~600 (for chlorophyll-a and DOX) to ~2100 (for tem-
530 perature and salinity) 0.1° cells in the Adriatic Sea. OBIS occurrence records that had
531 undergone expert review were extracted for these cells to increase observation reliability
532 (at the expense of their quantity). The extracted records between 2015 and 2018 were
533 47 for *Sepia officinalis*, 189 for *Merluccius merluccius*, 166 for *Mullus barbatus*, 39 for
534 *Sardina pilchardus*, 30 for *Parapenaeus longirostris*, 28 for *Solea solea*, 40 for *Squilla*
535 *mantis*, and 27 for *Engraulis encrasicolus*. These observations were distributed across
536 the species' Adriatic habitats (Figure 1). Although they were theoretically unsuitable for
537 building a detailed model, they were useful for a macroscopic pattern-change analysis of
538 species distributions, in agreement with other ENM approaches that use even a lower num-
539 ber of observations to trace viable environmental envelopes for pattern analyses (Kaschner

et al., 2006; Rees, 2008; Ready et al., 2010; Kaschner et al., 2011; Coro et al., 2016a).

3.1. Model consistency

3.1.1. Variable selection and model optimisation

Our feature selection criterion was evaluated using the Kuenm R package (Cobos et al., 2019), which also allowed us to fine-tune the models. This software exhaustively tests the performance of MaxEnt with multiple sets of environmental parameters and finds the optimal configuration of (i) the analytical form of h - among linear, quadratic, product, threshold, hinge, and their combinations (*feature classes*) - and (ii) a penalty factor on the β vector (*regularisation multiplier*) (Merow et al., 2013; Morales et al., 2017). Kuenm allows selecting the optimal model based on the highest Akaike Information Criterion value (AIC) calculated on a test set. To select the optimal parametrisations of our 2015-2018 models, several sets of environmental variables were prepared and evaluated in two ways: (i) on the entire training set (self-performance) and (ii) based on the average AIC over ten randomly extracted observation sets, with an 80-20% training-test set ratio for each extraction and considering only models with omission rate below 5%. The prepared sets of environmental variables included the entire set, the 95% *percent contribution*-based set (Section 2.3), and ten randomly chosen subsets.

The Kuenm evaluation estimated that the optimal regularisation multipliers for all analysed species ranged around 1. Thus, this parameter was fixed to 1 for all models for simplicity, i.e. no penalty was set on β . Moreover, both self-performance and 80-20% validation indicated that the optimal set of environmental variables was the one obtained using a 95% threshold *percent contribution* from the maximum contribution. Finally, using a complex h function that combined all feature classes was optimal for 80-20% valida-

tion and also gained high self-accuracy performance. The average AIC over all tests was ~990, whereas the average optimal models' AIC was ~860. These results likely derive from the fact that our selection criterion discards the predictor variables that bring poor and potentially confounding information to the model. Moreover, using complex feature classes reduced the over-fitting bias (Section 2.3) and thus likely increased validation performance.

As a further evaluation step, the *Receiver Operating Characteristic* (ROC) curve was traced for each optimal model to conduct a sensitivity analysis. This analysis calculated the true-positive rate and the false-positive rate using various decision-thresholds on the model output. Consequently, all optimal models were verified to achieve an *Area Under the Curve* (AUC) (i.e., the integral of the ROC curve) over 0.95. Specifically, AUC was averagely 0.96 [0.954;0.97] for the optimal models, and 0.83 [0.78;0.95] for sub-optimal models. This property guaranteed that the probability distributions simulated by each model were significantly higher on species-presence locations than on random locations. All these quality checks aimed to optimise model robustness in a context of scattered environmental data and few observation data.

It is worth noting that using AIC as a selection criterion can be prone to criticisms, especially because AIC tends to select models with a higher number of parameters among equal-likelihood models (Guthery et al., 2005; Arnold, 2010). However, issues especially arise if AIC were used (i) as the only selection criterion, (ii) without adding prior information to guide selection, and (iii) to build models that pretend to assess ecological reality (Zhang et al., 2018; Reside et al., 2019; Roy-Dufresne et al., 2019). Therefore, our use of AIS, through Kuenm, can be tolerated because we (i) did not assume the optimal models

586 to be punctually reliable, but generally reliable to assess macroscopic changes when com-
587 pared to each other, (ii) used a prior condition to evaluate only the models with omission
588 rates below 5%, (iii) forcibly introduced a further parametrisation that involved the 95%
589 percent contribution-based set; (iv) added sensitivity analysis to assess model validity fur-
590 ther; (v) checked model consistency through comparison with AquaMaps; (vi) introduced
591 constraints to avoid over-fitting. Indeed, the optimal models did not use the highest number
592 of environmental parameters and complex regularisation and penalty conditions.

593 The optimal parametrisations estimated for the FS 2015-2018 models were also used
594 for the FS 2019 and FS 2020 projections. The resulting optimal distributions are reported
595 in Figure 2.

596 3.1.2. Comparison with AquaMaps

597 The dissimilarity between our maps and AquaMaps 2019 was reasonably low, i.e., av-
598 eraging below 20% (19.14%, Table 1). Furthermore, a *fair* kappa agreement (according
599 to Landis and Koch classification, Landis and Koch (1977)) occurred for 81.3% of the
600 comparisons. The greatest discrepancy, corresponding to *slight* agreement, was found for
601 *Engraulis encrasicolus* and *Merluccius merluccius*. For these species (Figures 2-h and
602 -b), AquaMap 2019 extended more into south Adriatic. As for AquaMaps 2050, the IPCC
603 SRES A2 scenario was found to be significantly distant from our distributions, with a
604 ~30% average discrepancy and *poor/marginal* agreement with 87.5% of the distributions.
605 The highest similarity - with *moderate* kappa agreement - occurred for *Squilla mantis*
606 (19.2% discrepancy vs FS 2015-2018, 17.57% vs FS 2019, and 19.07% vs FS 2020). The
607 FS models indicated that this species had a stable habitat concentrated in northern Adriatic,
608 whereas AquaMaps 2019 estimated a possible presence in south Adriatic. Notably, OBIS

609 does not report expert-verified occurrences of *Squilla mantis* in south Adriatic, which en-
610 forces the consistency of our model.

611 Overall, this assessment indicates that our distributions generally agreed with an in-
612 dependent reference model (AquaMaps 2019) and were far from an unlikely scenario
613 (AquaMaps 2050). Thus, despite the poor data, the predictions of our models were not
614 poor, which permitted us to conduct further analyses and extract general patterns over the
615 Adriatic.

616 3.2. Habitat change classification

617 Based on the discrepancy (Table 1) and the suitability score (Table 2) calculations,
618 detailed habitat gain and loss trends were traced per species. In particular, *Sepia of-*
619 *ficinalis* habitat expanded in 2020 with respect to both 2015-2018 (+3.95%) and 2019
620 (+0.14%) with significant discrepancy (12.36% vs. 2015-2018 and 7.18% vs. 2019) (Fig-
621 ure 2-a). Distributional differences were found off the Apulian coasts and in the south
622 Balkans. The FS 2020 distribution was also similar to AquaMaps 2019, with *substantial*
623 kappa agreement, because both the distributions indicated extension towards south-east
624 and south-west. In northern Adriatic, the FS 2020 map presented a similar distribution
625 to the other FS maps, with *substantial* kappa agreement. This distribution was differ-
626 ent from AquaMaps 2050 (24.72% discrepancy), which predicted habitat loss throughout
627 south Adriatic. Overall, this analysis indicates habitat gain for this species in 2020.

628 *Merluccius merluccius* habitat expanded in 2020 with respect to 2015-2018 (+5.68%)
629 but minimally lost habitat with respect to 2019 (-0.36%) (Figure 2-b). The discrepancy vs
630 2019 (5.89%) was lower than vs 2015-2018 (17.82%). The similarity between FS 2020
631 and FS 2019 was due to minimal differences in the south-eastern Adriatic. Furthermore,

632 FS 2019 reported habitat gain (+7.04%) against FS 2015-2018, which indicated an increas-
633 ing habitat extension trend over the years. The greatest discrepancy between FS 2020 and
634 AquaMaps 2019 was in the south Adriatic, where AquaMaps reported high suitability.
635 The FS 2020 distribution was also different from AquaMaps 2050 (41.03% discrepancy)
636 due to the AquaMaps-predicted habitat loss throughout south Adriatic in 2050. Overall,
637 this analysis suggests habitat *gain* for this species in 2020 because its habitat substantially
638 expanded with respect to 2015-2018 and was similar to a habitat-favourable 2019.

639 Similarly, *Mullus barbatus* habitat expanded in 2020 with respect to 2015-2018 (+3.38%)
640 and slightly lost habitat with respect to 2019 (-1.94%) (Figure 2-c). The discrepancy vs
641 2019 (9.20%) was lower than vs 2015-2018 (16.24%). The similarity between FS 2020
642 and FS 2019 was due to minimal differences in middle Adriatic. Furthermore, FS 2019
643 resulted in habitat gain (+7.61%) against FS 2015-2018, which indicated an increasing
644 habitat extension trend over the years. The FS 2020 was also similar to AquaMaps 2019
645 (19.6% discrepancy and *moderate* agreement) because both models reported high suit-
646 ability for south Adriatic. For this reason, FS 2020 was different from AquaMaps 2050
647 (27.42% discrepancy and *poor* agreement), which foresaw habitat loss in south Adriatic.
648 Overall, this analysis indicates habitat *gain* for *Mullus barbatus* in 2020 because its habi-
649 tat substantially expanded with respect to 2015-2018 and was similar to an advantageous
650 2019.

651 *Sardina pilchardus* habitat expanded with respect to 2015-2018 (+4.6%) but substan-
652 tially lost habitat with respect to 2019 (-5.46%) (Figure 2-d). The discrepancy between FS
653 2020 and FS 2019 (29.6%) was concentrated off Apulian coasts (with gain in 2020) and in
654 the Balkans (with gain in 2019). Furthermore, FS 2019 reported habitat gain (+4.31%) vs

655 2015-2018 especially in south-western Adriatic and off central Italian coasts. Thus, habi-
656 tat trend was not stable, and the FS 2020 habitat suitability patterns changed with respect
657 to FS 2015-2018 and FS 2019. Due to the high suitability reported in south Adriatic, all
658 FS distributions had *moderate* agreement with AquaMaps 2019. The discrepancy between
659 FS 2020 and AquaMaps 2050 (20.89%) was lower than the one of the previous species
660 because also AquaMaps 2050 foresaw suitable habitat in 2050 in south Adriatic. Overall,
661 this analysis indicates habitat *change* for *Sardina pilchardus* in 2020 because no definite
662 trend and pattern was present across the models.

663 Similarly, *Parapenaeus longirostris* habitat expanded with respect to 2015-2018 (+8.33%)
664 but substantially lost habitat with respect to 2019 (-7.04%) (Figure 2-e). The discrepancy
665 between FS 2020 and FS 2019 (20.83%) was concentrated in the south and middle Adri-
666 atic (with gain in 2019). In the same areas, FS 2019 reported substantial habitat gain
667 (+14.87%) vs 2015-2018. Thus, habitat trend was unstable since the FS 2020 habitat suit-
668 ability patterns were substantially different with respect to FS 2015-2018 and FS 2019.
669 All FS distributions had *moderate* kappa agreement with AquaMaps 2019 due to the high
670 habitat suitability AquaMaps indicated in south Adriatic. In contrast, since AquaMaps
671 2050 indicated great habitat loss in south Adriatic, the discrepancy with FS distributions
672 was large (42.37% average). Overall, this analysis indicates habitat *change* for *Parape-*
673 *naeus longirostris* in 2020 because no definite trend and pattern was present across the
674 models.

675 *Solea solea* slightly gained habitat with respect to 2015-2018 (+0.5%) and presented
676 stable habitat suitability with respect to 2019 (Figure 2-f). The discrepancy between FS
677 2020 and FS 2015-2018 (6.75%) was due to a slightly higher suitability area off Apulian

678 coasts by FS 2020. The habitat change trend was thus stable, and the similarity and the
679 kappa agreement between the FS 2020 and the other distribution was *substantial*. The
680 FS distributions also had *substantial* kappa agreement with AquaMaps 2019, with very
681 similar patterns throughout the Adriatic. Since AquaMaps 2050 foresaw great habitat loss
682 in south Adriatic (except for a small area in southern Balkans), its discrepancy with respect
683 to the FS distributions was high (34.63%). Overall, this analysis indicates *stable* habitat
684 for *Solea solea* from 2015-2018 to 2020.

685 *Squilla mantis* slightly gained habitat with respect to 2015-2018 (+0.36%) and slightly
686 lost habitat with respect to 2019 (-0.72%) (Figure 2-g). The discrepancy between FS
687 2020 and the other FS distributions was concentrated off the Apulian coasts. The habitat
688 change trend was overall stable, and kappa agreement between the FS 2020 and the other
689 distribution was *substantial*. The FS distributions also had *moderate* kappa agreement
690 with AquaMaps 2019, which reported habitat suitability for most of the Adriatic. Since
691 AquaMaps 2050 reported high probability areas in northern and middle Adriatic and off
692 northern Albanian coasts, kappa agreement with the FS maps was *moderate*. Overall,
693 *Solea solea* presented an overall *stable* habitat from 2015-2018 to 2020.

694 *Engraulis encrasicolus* presented stable habitat distribution with respect to 2015-2018
695 and a slight suitability loss with respect to 2019 (-1.15%) (Figure 2-h). The discrep-
696 ancy between FS 2020 and FS 2019 was due to a higher probability area off Albanian
697 coasts. The habitat change trend was overall stable, and the mutual similarity had *sub-*
698 *stantial* kappa agreement. The FS distributions also had *moderate* kappa agreement with
699 AquaMaps 2019, which presented a decreasing gradient from north to south. Since AquaMaps
700 2050 reported habitat loss for middle and south Adriatic, kappa agreement with the FS

701 maps was *poor*. Overall, *Engraulis encrasicolus* presented an approximately *stable* habi-
702 tat from 2015-2018 to 2020.

703 3.3. *Habitat change due to environmental parameter change*

704 The key driving parameters for habitat change in 2020 were identified through the
705 analysis of their *percent contributions* (Table 4). Notably, the MaxEnt parameter selection
706 corresponded to known environmental preferences of the studies species. For example,
707 *Mullus barbatus* lives in sandy, muddy bottoms near river mouths (Esposito et al., 2014),
708 and indeed its key parameters were bottom temperature and depth, but also chlorophyll-a
709 and DOX averages in the upper water column. *Sardina pilchardus* habitat-depth ranges
710 between 10 and 100 m (Santos et al., 2006), and indeed it was associated with bottom and
711 water-column averaged parameters. *Parapenaeus longirostris* is a deep-water species, and
712 its habitat was indeed highly dependent on depth. However, its distribution also depends
713 on temperature and DOX in the water column (Ardizzone et al., 1990) as confirmed by our
714 MaxEnt model.

715 The single-parameter charts of FS 2015-2018 - produced by MaxEnt after training -
716 were used to identify the most significant driving factors of the change (Figure 3). In addi-
717 tion, parameter quartiles were extracted to understand if variation trends could be identified
718 among the driving factors (Table 3). To enhance readability, only the parameter distribu-
719 tions that were sensitive to parameter change over the years, i.e., with probability density
720 variation over 0.05 - were reported in Figure 3. Other probability distributions indicated
721 non-significant variation in correspondence of the median parameter change over the years
722 (e.g., they reported a plateau over the variation range), and were omitted. Since this anal-
723 ysis was conducted on the optimal models, only the parameters that showed significant

percent contribution were analysed for each species' distribution.

As regards the species that expanded habitat, *Sepia officinalis* was mainly supported by a general decreasing trend, from 2015 to 2020, of average DOX (with median going from 234.1 to 213.7 $\mu\text{mol/kg}$, Table 3) and an increasing trend of bottom temperature over the years (with median rising from 14.15 to 14.32 °C, Table 3). These two parameters significantly contributed to the MaxEnt model, and their trends went towards maxima of the single-parameter densities (Figure 3-a). Change in the other parameters did not influence habitat gain and thus was not discussed. *Merluccius merluccius* and *Mullus barbatus* expanded habitat especially because of increasing bottom temperature trend and decreasing average chlorophyll-a over time (from 0.039 to 0.034 mg/m^3 , Table 3). These changes moved the habitat to higher MaxEnt probability values and consequently increased habitat gain (Figures 3-b and -c).

As regards the species that changed habitat, the inconstant trend of *Sardina pilchardus* was due to average DOX and average chlorophyll-a decrease (Table 3). This decrease changed habitat suitability in 2020 with respect to 2015-2018 (Figure 3-d), and also generated different patterns between the FS 2019 and 2020 distributions. Habitat change for *Parapenaeus longirostris* was mainly driven by surface temperature modulations (from 16.6 °C in 2015-2018 to 19.7 °C in 2019 and 18.4 °C in 2020, Table 3) and surface DOX modulations (from 228.36 $\mu\text{mol/kg}$ in 2015-2018 to 227.8 $\mu\text{mol/kg}$ in 2019 and 214.7 $\mu\text{mol/kg}$ in 2020, Table 3). For this species, this parameter combination resulted in a less favourable habitat in 2020 than the previous years (Figure 3-e).

The species with stable habitat distributions presented a robust response to environmental change, and no parameter could be highlighted over the others.

747 3.4. Environmental parameter relation with climate change and COVID-19 pandemic

748 The parameters that principally drove distribution changes - i.e., temperature, chlorophyll-
749 a, and DOX - were analysed to understand if their change depended on inter-annual cli-
750 matic variations, general climate change trends or the COVID-19 pandemic (Table 5).

751 The general change of temperature positively affected the distributions of *Sepia offic-*
752 *inalis*, *Merluccius merluccius*, *Mullus barbatus*, but negatively the one of *Parapenaeus*
753 *longirostris*. Despite the cooling effect of La Niña since August 2020 - which mainly af-
754 fected surface temperature - global temperature increased up to 1.2 °C above pre-industrial
755 value (DownToEarth; United Nations, 2021a; World Meteorological Organization, 2021).

756 Similarly, the general decrease of DOX positively affected the habitat of *Sepia of-*
757 *ficinalis*, but negatively the habitats of *Sardina pilchardus* and *Parapenaeus longirostris*.
758 Although in 2020 DOX increased in several world areas, as the consequence of the qual-
759 ity improvement of coastal environments during the pandemic (Arif et al., 2020), in the
760 Adriatic Sea the trend has been strongly decreasing in the last two decades (Kralj et al.,
761 2019b). The Adriatic has a generally increasing DOX gradient from north to south conse-
762 quent to its water circulation, a decreasing nutrient concentration provided by rivers, and
763 a higher phytoplankton development in northern regions (especially in autumn and win-
764 ter) (Zavatarelli et al., 1998). The overall average DOX decrease trend is probably due to a
765 general DOX depletion at the Adriatic Sea floor. DOX level correlates with plankton respi-
766 ration and benthic oxygen consumption, which has been exceeding the oxygen produced
767 by microalgae and the one coming from oxygenated water (Kralj et al., 2019b; Lipizer
768 et al., 2014). This condition has been assessed as being a probable consequence of bottom
769 temperature and salinity increase due to climate change (Marasović et al., 2005; Lipizer

et al., 2014; Kralj et al., 2019a), and indeed was never observed before 1984 (Justić et al., 1987).

Conversely, the strong chlorophyll-a decrease in 2020 - i.e., -6% in the water column, -50% at the sea bottom, and -14% at the surface than 2019, based on the Argo data (Table 3) - could be correlated with the COVID-19 pandemic. Although this correlation cannot be demonstrated with our data, some supporting conjectures can be reported from other studies. Chlorophyll-a is indeed one of the main indicators of ocean productivity and is an integral part of the carbon cycle and oxygen production. The carbon cycle indeed depends on carbon dioxide consumption during photosynthetic primary production and inorganic carbon production during biomineralisation. The global balance of the natural carbon cycle implies that a large decrease of carbon dioxide (CO₂) in the atmosphere likely corresponds to a lower chlorophyll-a level because of the lower demand for CO₂ uptake (Shehhi and Samad, 2021). In 2020, a 7% reduction in the global carbon dioxide emissions was measured from satellite and *in situ* estimates due to big industry closure in several world countries with high industrial activity and large population (Le Quéré et al., 2020). As a probable consequence (Adwibowo, 2020; Mishra et al., 2020), a consistent decrease of chlorophyll-a was observed in many areas throughout 2020. For example, a 123 tonne reduction of CO₂ emission in south China corresponded to a measured 5% reduction of chlorophyll-a during the pandemic (Shehhi and Samad, 2021). This phenomenon was also observed in north Europe, South Korea, south-east United States, the Pacific Ocean, Middle East, western Africa, and south-east Australia. Thus, the chlorophyll-a decrease was probably a global phenomenon correlated with anthropogenic activity reduction (Shehhi and Samad, 2021).

793 Thus, our analysis indicates that the COVID-19 pandemic likely resulted in modify-
794 ing three species habitats among those studied: it positively affected the distributions of
795 *Merluccius merluccius* and *Mullus barbatus*, but negatively the one of *Sardina pilchardus*.

796 **4. Discussion and Conclusions**

797 This paper has presented an analysis of habitat change in 2020 with respect to the pre-
798 vious years (2015-2018 aggregated and 2019), based on floating sensor information and
799 species occurrence records from the OBIS data collection. Our experiment estimated the
800 habitat of 8 commercial species of the Adriatic Sea over this period. The produced eco-
801 logical niche distributions were sufficiently reliable when compared to those produced by
802 an independent model. They were similar to a model based on 2019 environmental con-
803 ditions (AquaMaps 2019) and very distant from a model based on a currently improbable
804 environmental scenario (AquaMaps 2050).

805 Our distributions were suitable for a pattern analysis to investigate if habitat change
806 depended on climate change or the COVID-19 pandemic. The main parameters that influ-
807 enced habitat change were the general increase of temperature and the overall decrease of
808 dissolved oxygen and chlorophyll-a. Although the observed temperature and DOX trends
809 depend on climate change, the chlorophyll-a decrease in 2020 was likely a consequence
810 of the COVID-19 pandemic.

811 Although some species - *Solea solea*, *Squilla mantis*, and *Engraulis encrasicolus* -
812 were not significantly affected by these changes, heterogeneous effects on the other species
813 habitat were observed. The increasing temperature and decreasing DOX trends - i.e., the
814 potential effects of climate change - negatively affected the distribution of *Parapenaeus*

815 *longirostris* by making its habitat overall unstable and less suitable in 2020 than in 2019.
816 This potential negative dependency on climate change finds confirmation by several stud-
817 ies on this species (Ungaro and Gramolini, 2006; Colloca et al., 2014; Sbrana et al., 2019;
818 Quattrocchi et al., 2020). Conversely, these trends favoured *Sepia officinalis* and extended
819 its potential habitat, in agreement with other studies that analysed its response to the single
820 parameter changes (Palmegiano and d'Apote, 1983; Capaz et al., 2017).

821 The potential coupling between climate change and COVID-19 - manifested as a
822 simultaneous decreasing trend of DOX and chlorophyll-a - negatively affected the dis-
823 tribution of *Sardina pilchardus*. Other studies have also reported habitat instability of
824 this species' habitat as the consequence of the variation of these parameters (Sinovčić,
825 2001; Ganas, 2009). However, the combination of rising temperature and decreasing
826 chlorophyll-a positively affected the habitats of *Merluccius merluccius* and *Mullus barba-*
827 *tus*. This observation agrees with parameter-specific indications by other studies (Gucu
828 and Bingel, 2011; García-Rodríguez et al., 2011; Sabates et al., 2015; Sion et al., 2019).
829 These two species were the major beneficiary of the two parameter trend combination.
830 Thus, reduced anthropogenic stress on ecosystems in 2020 was beneficial for some species'
831 habitats.

832 4.1. Reusability and limitations of the approach

833 Our approach predicted potential general consequences of climate change on species
834 habitat and its coupling with the COVID-19 pandemic. In this view, it can be useful for
835 integrated environmental assessments (Antunes and Santos, 1999; Kristensen, 2004). For
836 example, it can be combined with human activity analysis and when estimating available
837 biomass, and can be used in models that predict risk of regime shift caused by habitat loss

(deyoung et al., 2008; Graham et al., 2015; Wernberg et al., 2016). Notably, the potential effects of reduced fishing activity - due to sanitary restrictions and market closure - on habitat distributions are yet unclear. Only a 10% reduction of fishing hours with respect to the 2019 level has been estimated globally (for large and small scale fisheries) (Clavelle, 2020; WWF, 2020). Furthermore, the overall fishing activity reduction was just 4% in the Italian seas (Clavelle, 2020). Such a low reduction possibly had minor effects on the habitat distributions of our analysed species and will be the subject of our future investigations. Our approach is also general enough to be applied to other species and areas. To this aim, our workflow uses FAIR data that have a global-scale coverage. Furthermore, our software is open source, and all data are reported under the ESRI-grid format (see Supplementary Material). Specifically, the optimal MaxEnt models and the data are all available as raster ESRI-grid files in the repository linked in the Supplementary Material, within the "Phase 4 - MaxEnt Re-application/MaxEnt Distributions and Statistics" folder, for re-use in GIS software and other experiments.

The main limitation of our experiment is the low amount of data used, due to current data availability, which was partially compensated by accurate data selection and model optimisation. Although the proposed Adriatic-scale pattern analysis is reliable enough to extract habitat change trends, the produced maps cannot be considered punctually reliable (Queiroz et al., 2021). Conducting a precise analysis will require collecting, collating, and analysing a massive amount of data that will be available only years after the end of the pandemic. Nevertheless, data-poor approaches like ours can predict realistic macroscopic patterns and indicate priority directions for investigating species modifications in the search for confirmation or confutation of the reported results (Coro et al., 2015b,

2016a). In this view, our model allows looking ahead to the possible significant modifications that will possibly be observed in the Adriatic in the following years due to the impact of the combined action of the COVID-19 pandemic and climate change on species distributions. Small-scale reliability can also be enhanced in our model when marine environmental data and species records will be more dense and uniform in the study area. Several initiatives are promoting the collection of these data (EU Commission, 2020a; Snapshot-CNR, 2020; EU Commission, 2020b), but they are ongoing and main address regional scales. These data will be a fundamental source of information to repeat our analysis and validate its predictions. We believe that these activities are justified to understand the effects of natural and man-made pressure on marine ecosystems in current and future scenarios. Our study also confirmed that in order to realise the UN Decade on Ecosystem Restoration motto "the science we need for the ocean we want" (United Nations, 2021b) an Open Science approach can be successful.

Supplementary Material

Experimental data and source code are publicly available on the D4Science e-Infrastructure <https://data.d4science.net/WLNn>

Acknowledgments

The authors acknowledge Enrico Nicola Armelloni and Giuseppe Scarcella for indications about Adriatic fisheries. This research was partially funded by the SNAPSHOT project of the National Research Council of Italy (CNR) and by the Blue Cloud EU project (Grant Agreement No.862409).

882 References

- 883 Adwibowo, A., 2020. Does social distancing have an effect on water quality?: An evidence
884 from chlorophyll-a level in the water of populated southeast asian coasts. <https://www.preprints.org/manuscript/202005.0091/v1/download>.
885
- 886 Alvera-Azcárate, A., Barth, A., Rixen, M., Beckers, J.M., 2005. Reconstruction of incom-
887 plete oceanographic data sets using empirical orthogonal functions: application to the
888 adriatic sea surface temperature. *Ocean Modelling* 9, 325–346.
- 889 Angeletti, L., Prampolini, M., Foglini, F., Grande, V., Taviani, M., 2020. Cold-water coral
890 habitat in the bari canyon system, southern adriatic sea (mediterranean sea), in: *Seafloor*
891 *Geomorphology as Benthic Habitat*. Elsevier, pp. 811–824.
- 892 Antunes, P., Santos, R., 1999. Integrated environmental management of the oceans. *Eco-*
893 *logical Economics* 31, 215–226.
- 894 AquaMaps, 2020. AquaMaps Web site. www.aquamaps.org.
- 895 Araujo, M.B., Naimi, B., 2020. Spread of sars-cov-2 coronavirus likely to be constrained
896 by climate. doi:10.1101/2020.03.12.20034728. preprint.
- 897 Ardizzone, G., Gravina, M., Belluscio, A., Schintu, P., 1990. Depth-size distribution
898 pattern of *parapenaeus longirostris* (lucas, 1846)(decapoda) in the central mediterranean
899 sea. *Journal of Crustacean Biology* 10, 139–147.
- 900 Argo, 2000. Argo float data and metadata from global data assembly centre (argo gdac).
901 SEANOE, <https://doi.org/10.17882/42182>.

- 902 Arif, M., Kumar, R., Parveen, S., Verma, N., 2020. Reduction in water pollution in yamuna
903 river due to lockdown under covid-19 pandemic. *The Pharma Innovation Journal* 9, 84–
904 89.
- 905 Arnold, T.W., 2010. Uninformative parameters and model selection using akaike’s infor-
906 mation criterion. *The Journal of Wildlife Management* 74, 1175–1178.
- 907 Ashraf, U., Peterson, A.T., Chaudhry, M.N., Ashraf, I., Saqib, Z., Rashid Ahmad, S., Ali,
908 H., 2017. Ecological niche model comparison under different climate scenarios: a case
909 study of olea spp. in asia. *Ecosphere* 8, e01825.
- 910 Assante, M., Candela, L., Castelli, D., Cirillo, R., Coro, G., Frosini, L., Lelii, L., Man-
911 giacrappa, F., Pagano, P., Panichi, G., et al., 2019. Enacting open science by d4science.
912 *Future Generation Computer Systems* 101, 555–563.
- 913 Azzolin, M., Arcangeli, A., Cipriano, G., Crosti, R., Maglietta, R., Pietroluongo, G.,
914 Saintingan, S., Zampollo, A., Fanizza, C., Carlucci, R., 2020. Spatial distribution mod-
915 elling of striped dolphin (*stenella coeruleoalba*) at different geographical scales within
916 the eu adriatic and ionian sea region, central-eastern mediterranean sea. *Aquatic Con-*
917 *servation: Marine and Freshwater Ecosystems* 30, 1194–1207.
- 918 Baker, R.E., Peña, J.M., Jayamohan, J., Jérusalem, A., 2018. Mechanistic models versus
919 machine learning, a fight worth fighting for the biological community? *Biology letters*
920 14, 20170660.
- 921 Bargain, A., Marchese, F., Savini, A., Taviani, M., Fabri, M.C., 2017. Santa maria di leuca
922 province (mediterranean sea): Identification of suitable mounds for cold-water coral

923 settlement using geomorphometric proxies and maxent methods. *Frontiers in Marine*
 924 *Science* 4, 338.

925 Barth, A., Alvera-Azcárate, A., Troupin, C., Ouberdous, M., Beckers, J.M., 2010. A
 926 web interface for gridding arbitrarily distributed in situ data based on data-interpolating
 927 variational analysis (diva). *Advances in Geosciences* 28, 29–37.

928 Ben Rais Lasram, F., Guilhaumon, F., Albouy, C., Somot, S., Thuiller, W., Mouillot, D.,
 929 2010. The mediterranean sea as a ‘cul-de-sac’ for endemic fishes facing climate change.
 930 *Global Change Biology* 16, 3233–3245.

931 Bennett, A.F., 1992. *Inverse methods in physical oceanography*. Cambridge university
 932 press.

933 Blackford, J., 2002. The influence of microphytobenthos on the northern adriatic ecosys-
 934 tem: a modelling study. *Estuarine, Coastal and Shelf Science* 55, 109–123.

935 Brown, C., Fulton, E., Hobday, A., Matear, R., Possingham, H., Bulman, C., Christensen,
 936 V., Forrest, R., Gehrke, P., Gribble, N., et al., 2010. Effects of climate-driven primary
 937 production change on marine food webs: implications for fisheries and conservation.
 938 *Global Change Biology* 16, 1194–1212.

939 Candela, L., Castelli, D., Coro, G., Pagano, P., Sinibaldi, F., 2016. Species distribution
 940 modeling in the cloud. *Concurrency and Computation: Practice and Experience* 28,
 941 1056–1079.

942 Capaz, J.C., Tunnah, L., MacCormack, T.J., Lamarre, S.G., Sykes, A.V., Driedzic, W.R.,
 943 2017. Hypoxic induced decrease in oxygen consumption in cuttlefish (*sepia officinalis*)

944 is associated with minor increases in mantle octopine but no changes in markers of
 945 protein turnover. *Frontiers in physiology* 8, 344.

946 Capezzuto, F., Sion, L., Ancona, F., Carlucci, R., Carluccio, A., Cornacchia, L., Maiorano,
 947 P., Ricci, P., Tursi, A., D'Onghia, G., 2018. Cold-water coral habitats and canyons as
 948 essential fish habitats in the southern adriatic and northern ionian sea (central mediter-
 949 ranean). *Ecological Questions* 29, 9–23.

950 Chala, D., Roos, C., Svenning, J.C., Zinner, D., 2019. Species-specific effects of climate
 951 change on the distribution of suitable baboon habitats—ecological niche modeling of
 952 current and last glacial maximum conditions. *Journal of human evolution* 132, 215–
 953 226.

954 Chunco, A.J., Phimmachak, S., Sivongxay, N., Stuart, B.L., 2013. Predicting environ-
 955 mental suitability for a rare and threatened species (lao newt, *laotriton laoensis*) using
 956 validated species distribution models. *PLoS One* 8, e59853.

957 Clavelle, T., 2020. Global fisheries during COVID-
 958 19. [https://globalfishingwatch.org/data-blog/
 959 global-fisheries-during-covid-19/](https://globalfishingwatch.org/data-blog/global-fisheries-during-covid-19/).

960 Cobos, M.E., Peterson, A.T., Barve, N., Osorio-Olvera, L., 2019. kuenm: an r package for
 961 detailed development of ecological niche models using maxent. *PeerJ* 7, e6281.

962 Cohen, J., et al., 1960. A coefficient of agreement for nominal scales. *Educational and
 963 psychological measurement* 20, 37–46.

- 964 Coll, M., Santojanni, A., Palomera, I., Tudela, S., Arneri, E., 2007. An ecological model
965 of the northern and central adriatic sea: analysis of ecosystem structure and fishing
966 impacts. *Journal of Marine Systems* 67, 119–154.
- 967 Colloca, F., Mastrantonio, G., Lasinio, G.J., Ligas, A., Sartor, P., 2014. *Parapenaeus lon-*
968 *girostris* (lucas, 1846) an early warning indicator species of global warming in the cen-
969 tral mediterranean sea. *Journal of Marine Systems* 138, 29–39. URL: <https://www.sciencedirect.com/science/article/pii/S0924796313002133>,
970 doi:<https://doi.org/10.1016/j.jmarsys.2013.10.007>. the wrapping
971 up of the IDEADOS project: International Workshop on Environment, Ecosystems and
972 Demersal Resources, and Fisheries.
- 974 Coro, G., 2020. A global-scale ecological niche model to predict sars-cov-2 coronavirus
975 infection rate. *Ecological Modelling* 431, 109187.
- 976 Coro, G., Bove, P., 2022. A high-resolution global-scale model for covid-19 infection rate.
977 *ACM Transactions on Spatial Algorithms and Systems (TSAS)* 8, 1–24.
- 978 Coro, G., Candela, L., Pagano, P., Italiano, A., Liccardo, L., 2015a. Parallelizing the
979 execution of native data mining algorithms for computational biology. *Concurrency*
980 *and Computation: Practice and Experience* 27, 4630–4644.
- 981 Coro, G., Ellenbroek, A., Pagano, P., 2021. An open science approach to infer fishing
982 activity pressure on stocks and biodiversity from vessel tracking data. *Ecological Infor-*
983 *matics* 64, 101384.
- 984 Coro, G., Magliozzi, C., Ellenbroek, A., Kaschner, K., Pagano, P., 2016a. Automatic

985 classification of climate change effects on marine species distributions in 2050 using
 986 the aquamaps model. *Environmental and ecological statistics* 23, 155–180.

987 Coro, G., Magliozzi, C., Ellenbroek, A., Pagano, P., 2015b. Improving data quality to build
 988 a robust distribution model for *architeuthis dux*. *Ecological modelling* 305, 29–39.

989 Coro, G., Magliozzi, C., Vanden Berghe, E., Bailly, N., Ellenbroek, A., Pagano,
 990 P., 2016b. Estimating absence locations of marine species from data of scien-
 991 tific surveys in obis. *Ecological Modelling* 323, 61–76. URL: <https://www.sciencedirect.com/science/article/pii/S0304380015005761>,
 992 doi:<https://doi.org/10.1016/j.ecolmodel.2015.12.008>.

994 Coro, G., Pagano, P., Ellenbroek, A., 2013a. Automatic procedures to assist in manual
 995 review of marine species distribution maps, in: *International Conference on Adaptive
 996 and Natural Computing Algorithms*, Springer. pp. 346–355.

997 Coro, G., Pagano, P., Ellenbroek, A., 2013b. Combining simulated expert knowledge with
 998 neural networks to produce ecological niche models for *latimeria chalumnae*. *Ecological
 999 modelling* 268, 55–63.

1000 Coro, G., Pagano, P., Ellenbroek, A., 2014. Comparing heterogeneous distribution maps
 1001 for marine species. *GIScience & Remote Sensing* 51, 593–611.

1002 Coro, G., Pagano, P., Ellenbroek, A., 2018a. Detecting patterns of climate change in long-
 1003 term forecasts of marine environmental parameters. *International Journal of Digital
 1004 Earth* , 1–19.

1005 Coro, G., Pagano, P., Ellenbroek, A., 2020. Detecting patterns of climate change in long-
 1006 term forecasts of marine environmental parameters. *International Journal of Digital*
 1007 *Earth* 13, 567–585.

1008 Coro, G., Pagano, P., Napolitano, U., 2016c. Bridging environmental data providers and
 1009 seadatanet diva service within a collaborative and distributed e-infrastructure. *Bollettino*
 1010 *di Geofisica* , 23–25.

1011 Coro, G., Panichi, G., Scarponi, P., Pagano, P., 2017. Cloud computing in a distributed
 1012 e-infrastructure using the web processing service standard. *Concurrency and Computa-*
 1013 *tion: Practice and Experience* 29, e4219.

1014 Coro, G., Scarponi, P., Pagano, P., 2018b. Enhancing argo floats data re-usability. *Bollet-*
 1015 *tino di Geofisica* 53.

1016 Coro, G., Tasseti, A.N., Armelloni, E.N., Pulcinella, J., Ferrà, C., Sprovieri, M., Trincardi,
 1017 F., Scarcella, G., 2022. Covid-19 lockdowns reveal the resilience of adriatic sea fisheries
 1018 to forced fishing effort reduction. *Scientific Reports* 12, 1–14.

1019 Coro, G., Trumpy, E., 2020. Predicting geographical suitability of geothermal power
 1020 plants. *Journal of Cleaner Production* 267, 121874.

1021 Coro, G., Vilas, L.G., Magliozzi, C., Ellenbroek, A., Scarponi, P., Pagano, P., 2018c.
 1022 Forecasting the ongoing invasion of *lagocephalus sceleratus* in the mediterranean sea.
 1023 *Ecological Modelling* 371, 37–49.

1024 Coro, G., Webb, T.J., Appeltans, W., Bailly, N., Cattrijsse, A., Pagano, P.,
 1025 2015c. Classifying degrees of species commonness: North sea fish as a

1026 case study. *Ecological Modelling* 312, 272–280. URL: <https://www.sciencedirect.com/science/article/pii/S0304380015002392>,
1027
1028 doi:<https://doi.org/10.1016/j.ecolmodel.2015.05.033>.

1029 Corsi, F., de Leeuw, J., Skidmore, A., 2000. Modeling species distribution with GIS.
1030 *Research Techniques in Animal Ecology*. Columbia University Press, New York n/a,
1031 389–434.

1032 Deneu, B., Servajean, M., Bonnet, P., Botella, C., Munoz, F., Joly, A., 2021. Convolu-
1033 tional neural networks improve species distribution modelling by capturing the spatial
1034 structure of the environment. *PLOS Computational Biology* 17, e1008856.

1035 Depellegrin, D., Bastianini, M., Fadini, A., Menegon, S., 2020. The effects of covid-19
1036 induced lockdown measures on maritime settings of a coastal region. *Science of the*
1037 *Total Environment* 740, 140123.

1038 deyoung, B., Barange, M., Beaugrand, G., Harris, R., Perry, R.I., Scheffer, M., Werner,
1039 F., 2008. Regime shifts in marine ecosystems: detection, prediction and management.
1040 *Trends in Ecology & Evolution* 23, 402–409.

1041 Djakovac, T., Supić, N., Aubry, F.B., Degobbis, D., Giani, M., 2015. Mechanisms of
1042 hypoxia frequency changes in the northern adriatic sea during the period 1972–2012.
1043 *Journal of Marine Systems* 141, 179–189.

1044 DownToEarth, . Upper oceans hottest in 2020 despite lower emissions due to COVID-
1045 19 lockdowns. [www.downtoearth.org.in/news/climate-change/upper-oceans-hottest-in-](http://www.downtoearth.org.in/news/climate-change/upper-oceans-hottest-in-2020-despite-lower-emissions-due-to-covid-19-lockdowns-75056)
1046 [2020-despite-lower-emissions-due-to-covid-19-lockdowns-75056](http://www.downtoearth.org.in/news/climate-change/upper-oceans-hottest-in-2020-despite-lower-emissions-due-to-covid-19-lockdowns-75056).

1047 Dudík, M., Phillips, S., Schapire, R.E., 2005. Correcting sample selection bias in maxi-
 1048 mum entropy density estimation. *Advances in neural information processing systems*
 1049 18, 323–330.

1050 Durand, M., Fu, L.L., Lettenmaier, D.P., Alsdorf, D.E., Rodriguez, E., Esteban-Fernandez,
 1051 D., 2010. The surface water and ocean topography mission: Observing terrestrial sur-
 1052 face water and oceanic submesoscale eddies. *Proceedings of the IEEE* 98, 766–779.

1053 Elith, J., Graham, C.H., 2009. Do they? how do they? why do they differ? on finding
 1054 reasons for differing performances of species distribution models. *Ecography* 32, 66–
 1055 77.

1056 Elith, J., Phillips, S.J., Hastie, T., Dudík, M., Chee, Y.E., Yates, C.J., 2011. A statistical
 1057 explanation of maxent for ecologists. *Diversity and distributions* 17, 43–57.

1058 Esposito, V., Andaloro, F., Bianca, D., Natalotto, A., Romeo, T., Scotti, G., Castriota, L.,
 1059 2014. Diet and prey selectivity of the red mullet, *mullus barbatus* (pisces: Mullidae),
 1060 from the southern tyrrhenian sea: the role of the surf zone as a feeding ground. *Marine*
 1061 *Biology Research* 10, 167–178.

1062 EU Commission, 2020a. A European Green Deal. [https://ec.europa.eu/info/](https://ec.europa.eu/info/strategy/priorities-2019-2024/european-green-deal)
 1063 [strategy/priorities-2019-2024/european-green-deal](https://ec.europa.eu/info/strategy/priorities-2019-2024/european-green-deal).

1064 EU Commission, 2020b. Mission Starfish 2030: Restore our Ocean
 1065 and Waters. [https://ec.europa.eu/info/publications/](https://ec.europa.eu/info/publications/mission-starfish-2030-restore-our-ocean-and-waters_en)
 1066 [mission-starfish-2030-restore-our-ocean-and-waters_en](https://ec.europa.eu/info/publications/mission-starfish-2030-restore-our-ocean-and-waters_en).

1067 FAO, 2020. The State of Mediterranean and Black Sea Fisheries 2020. [https://doi.](https://doi.org/10.4060/cb2429en)
 1068 [org/10.4060/cb2429en](https://doi.org/10.4060/cb2429en).

1069 Friedlaender, A.S., Johnston, D.W., Fraser, W.R., Burns, J., Costa, D.P., et al., 2011.
 1070 Ecological niche modeling of sympatric krill predators around marguerite bay, west-
 1071 ern antarctic peninsula. *Deep Sea Research Part II: Topical Studies in Oceanography*
 1072 58, 1729–1740.

1073 Froese, R., Winker, H., Coro, G., Demirel, N., Tsikliras, A.C., Dimarchopoulou, D., Scar-
 1074 cella, G., Quaas, M., Matz-Lück, N., 2018. Status and rebuilding of european fisheries.
 1075 *Marine Policy* 93, 159–170.

1076 Ganas, K., 2009. Linking sardine spawning dynamics to environmental variabil-
 1077 ity. *Estuarine, Coastal and Shelf Science* 84, 402–408. URL: [https://www.](https://www.sciencedirect.com/science/article/pii/S0272771409003266)
 1078 [sciencedirect.com/science/article/pii/S0272771409003266](https://www.sciencedirect.com/science/article/pii/S0272771409003266),
 1079 doi:<https://doi.org/10.1016/j.ecss.2009.07.004>.

1080 Garcia, D.A., Amori, M., Giovanardi, F., Piras, G., Groppi, D., Cumo, F., De Santoli, L.,
 1081 2019. An identification and a prioritisation of geographic and temporal data gaps of
 1082 mediterranean marine databases. *Science of the total environment* 668, 531–546.

1083 García-Rodríguez, M., Fernández, A., Esteban, A., 2011. Biomass response to environ-
 1084 mental factors in two congeneric species of mullus, *m. barbatus* and *m. surmuletus*,
 1085 off catalano–levantine mediterranean coast of spain: a preliminary approach. *Animal*
 1086 *Biodiversity and Conservation* 34, 113–122.

- 1087 GEBCO, 2020. Gridded bathymetry data. [https://www.gebco.net/data_and_](https://www.gebco.net/data_and_products/gridded_bathymetry_data/)
1088 [products/gridded_bathymetry_data/](https://www.gebco.net/data_and_products/gridded_bathymetry_data/).
- 1089 GFCM, 2020. Geographical subareas of the General Fisheries Commission for the
1090 Mediterranean. <http://www.fao.org/gfcm/data/maps/gsas/en/>.
- 1091 Graham, N.A., Jennings, S., MacNeil, M.A., Mouillot, D., Wilson, S.K., 2015. Predicting
1092 climate-driven regime shifts versus rebound potential in coral reefs. *Nature* 518, 94–97.
- 1093 Grassle, J., 2000. The ocean biogeographic information system (obis): an on-line,
1094 worldwide atlas for accessing, modeling and mapping marine biological data in
1095 a multidimensional geographic context. *OCEANOGRAPHY-WASHINGTON DC-*
1096 *OCEANOGRAPHY SOCIETY*- 13, 5–7.
- 1097 Gucu, A., Bingel, F., 2011. Hake, *merluccius merluccius* L., in the northeastern mediter-
1098 ranean sea: a case of disappearance. *Journal of Applied Ichthyology* 27, 1001–1012.
- 1099 Guo, Q., Liu, Y., 2010. Modeco: an integrated software package for ecological niche
1100 modeling. *Ecography* 33, 637–642.
- 1101 Guthery, F.S., Brennan, L.A., Peterson, M.J., Lusk, J.J., 2005. Information theory in
1102 wildlife science: critique and viewpoint. *The Journal of Wildlife Management* 69, 457–
1103 465.
- 1104 Hengl, T., Sierdsema, H., Radović, A., Dilo, A., 2009. Spatial prediction of species'
1105 distributions from occurrence-only records: combining point pattern analysis, enfa and
1106 regression-kriging. *Ecological modelling* 220, 3499–3511.

- 1107 Huang, Y.P., Kao, L.J., Sandnes, F.E., 2008. Efficient mining of salinity and temperature
1108 association rules from argo data. *Expert Systems with Applications* 35, 59–68.
- 1109 Jones, M.C., Dye, S.R., Pinnegar, J.K., Warren, R., Cheung, W.W., 2012. Modelling
1110 commercial fish distributions: Prediction and assessment using different approaches.
1111 *Ecological Modelling* 225, 133–145.
- 1112 Justić, D., Legović, T., Rottini-Sandrini, L., 1987. Trends in oxygen content
1113 1911–1984 and occurrence of benthic mortality in the northern adriatic sea.
1114 *Estuarine, Coastal and Shelf Science* 25, 435–445. URL: <https://www.sciencedirect.com/science/article/pii/0272771487900357>,
1115 doi:[https://doi.org/10.1016/0272-7714\(87\)90035-7](https://doi.org/10.1016/0272-7714(87)90035-7).
- 1117 Kaschner, K., Ready, J., Agbayani, E., Kesner-Reyes, K., Rius-Barile, J., Eastwood, P.,
1118 South, A., Kullander, S., Rees, T., Watson, R., et al., 2011. Using 'aquamaps' for
1119 representing species distribution in regional seas, in: *Fisheries Centre Research Reports*.
1120 Fisheries Centre, University of British Columbia, pp. 17–21.
- 1121 Kaschner, K., Watson, R., Trites, A., Pauly, D., 2006. Mapping world-wide distributions of
1122 marine mammal species using a relative environmental suitability (res) model. *Marine*
1123 *Ecology Progress Series* 316, 285–310.
- 1124 Kemp, P.S., Froese, R., Pauly, D., 2020. Covid-19 provides an opportunity to advance
1125 a sustainable uk fisheries policy in a post-brexite brave new world. *Marine Policy* 120,
1126 104114.
- 1127 Kralj, M., Lipizer, M., Čermelj, B., Celio, M., Fabbro, C., Brunetti, F., Francé, J., Mozetič,

1128 P., Giani, M., 2019a. Hypoxia and dissolved oxygen trends in the northeastern adriatic
 1129 sea (gulf of trieste). *Deep Sea Research Part II: Topical Studies in Oceanography* 164,
 1130 74–88.

1131 Kralj, M., Lipizer, M., Čermelj, B., Celio, M., Fabbro, C., Brunetti, F., Francé,
 1132 J., Mozetič, P., Giani, M., 2019b. Hypoxia and dissolved oxygen trends
 1133 in the northeastern adriatic sea (gulf of trieste). *Deep Sea Research Part*
 1134 *II: Topical Studies in Oceanography* 164, 74–88. URL: <https://www.sciencedirect.com/science/article/pii/S096706451930013X>,
 1135 doi:<https://doi.org/10.1016/j.dsr2.2019.06.002>. revisiting the
 1136 Eastern Mediterranean: Recent knowledge on the physical, biogeochemical and
 1137 ecosystemic states and trends (Volume I).

1139 Kristensen, P., 2004. The dpsir framework, european topic centre on water. European
 1140 Environment Agency , 1–10.

1141 Landis, J.R., Koch, G.G., 1977. The measurement of observer agreement for categorical
 1142 data. *biometrics* , 159–174.

1143 Le Quéré, C., Jackson, R.B., Jones, M.W., Smith, A.J., Abernethy, S., Andrew, R.M., De-
 1144 Gol, A.J., Willis, D.R., Shan, Y., Canadell, J.G., et al., 2020. Temporary reduction in
 1145 daily global co₂ emissions during the covid-19 forced confinement. *Nature Climate*
 1146 *Change* 10, 647–653.

1147 Lipizer, M., Partescano, E., Rabitti, A., Giorgetti, A., Crise, A., 2014. Qualified temper-
 1148 ature, salinity and dissolved oxygen climatologies in a changing adriatic sea. *Ocean*
 1149 *Science* 10, 771–797.

- 1150 Magliozzi, C., Coro, G., Grabowski, R.C., Packman, A.I., Krause, S., 2019. A multiscale
1151 statistical method to identify potential areas of hyporheic exchange for river restoration
1152 planning. *Environmental Modelling & Software* 111, 311–323.
- 1153 Marasović, I., Ninčević, Ž., Kušpilić, G., Marinović, S., Marinov, S., 2005. Long-term
1154 changes of basic biological and chemical parameters at two stations in the middle adri-
1155 atic. *Journal of Sea Research* 54, 3–14.
- 1156 Menchetti, M., Guéguen, M., Talavera, G., 2019. Spatio-temporal ecological niche mod-
1157 elling of multigenerational insect migrations. *Proceedings of the Royal Society B* 286,
1158 20191583.
- 1159 Merow, C., Smith, M.J., Silander Jr, J.A., 2013. A practical guide to maxent for modeling
1160 species' distributions: what it does, and why inputs and settings matter. *Ecography* 36,
1161 1058–1069.
- 1162 Mishra, D.R., Kumar, A., Muduli, P.R., Equeenuddin, S.M., Rastogi, G., Acharyya, T.,
1163 Swain, D., 2020. Decline in phytoplankton biomass along indian coastal waters due
1164 to covid-19 lockdown. *Remote Sensing* 12. URL: [https://www.mdpi.com/](https://www.mdpi.com/2072-4292/12/16/2584)
1165 [2072-4292/12/16/2584](https://www.mdpi.com/2072-4292/12/16/2584), doi:10.3390/rs12162584.
- 1166 Morales, N.S., Fernández, I.C., Baca-González, V., 2017. Maxent's parameter configu-
1167 ration and small samples: are we paying attention to recommendations? a systematic
1168 review. *PeerJ* 5, e3093.
- 1169 Muscarella, R., Galante, P.J., Soley-Guardia, M., Boria, R.A., Kass, J.M., Uriarte, M.,
1170 Anderson, R.P., 2014. *Enm eval: An r package for conducting spatially independent*

1171 evaluations and estimating optimal model complexity for maxent ecological niche mod-
 1172 els. *Methods in ecology and evolution* 5, 1198–1205.

1173 O'Brien, P.C., 1980. The quartiles of the maximum entropy distribution. *Economics*
 1174 *Letters* 6, 49–52.

1175 OSGeo, 2019. GDAL - Geospatial Data Abstraction Library. [https://www.gdal.](https://www.gdal.org/)
 1176 [org/](https://www.gdal.org/).

1177 Palmegiano, G., d'Apote, M., 1983. Combined effects of temperature and salinity on
 1178 cuttlefish (*sepia officinalis* l.) hatching. *Aquaculture* 35, 259–264.

1179 Pearson, R.G., 2007. Species' distribution modeling for conservation educators and prac-
 1180 titioners. *Synthesis. American Museum of Natural History* 50, 54–89.

1181 Peterson, A.T., 2001. Predicting Species' Geographic Distributions Based on Ecological
 1182 Niche Modeling. *The Condor* 103, 599–605. URL: [https://doi.org/10.1093/](https://doi.org/10.1093/condor/103.3.599)
 1183 [condor/103.3.599](https://doi.org/10.1093/condor/103.3.599), doi:10.1093/condor/103.3.599.

1184 Peterson, A.T., 2003. Predicting the geography of species' invasions via ecological niche
 1185 modeling. *The quarterly review of biology* 78, 419–433.

1186 Peterson, T., Papeş, M., Eaton, M., 2007. Transferability and model evaluation in ecolog-
 1187 ical niche modeling: a comparison of garp and maxent. *Ecography* 30, 550–560.

1188 Phillips, S., Dudik, M., Schapire, R., 2021. Maxent software for modeling species niches
 1189 and distributions (Version 3.4.1). [http://biodiversityinformatics.amnh.](http://biodiversityinformatics.amnh.org/open_source/maxent/)
 1190 [org/open_source/maxent/](http://biodiversityinformatics.amnh.org/open_source/maxent/).

- 1191 Phillips, S.J., Anderson, R.P., Dudík, M., Schapire, R.E., Blair, M.E., 2017. Opening the
1192 black box: An open-source release of maxent. *Ecography* 40, 887–893.
- 1193 Phillips, S.J., Anderson, R.P., Schapire, R.E., 2006a. Maximum entropy modeling of
1194 species geographic distributions. *Ecological Modelling* 190, 231–259.
- 1195 Phillips, S.J., Anderson, R.P., Schapire, R.E., 2006b. Maximum entropy mod-
1196 eling of species geographic distributions. *Ecological Modelling* 190, 231 –
1197 259. URL: [http://www.sciencedirect.com/science/article/pii/](http://www.sciencedirect.com/science/article/pii/S030438000500267X)
1198 [S030438000500267X](http://www.sciencedirect.com/science/article/pii/S030438000500267X).
- 1199 Phillips, S.J., Dudík, M., 2008. Modeling of species distributions with maxent: new ex-
1200 tensions and a comprehensive evaluation. *Ecography* 31, 161–175.
- 1201 Quattrocchi, F., Fiorentino, F., Lauria, V., Garofalo, G., 2020. The increasing tempera-
1202 ture as driving force for spatial distribution patterns of *parapenaeus longirostris* (lucas
1203 1846) in the strait of sicily (central mediterranean sea). *Journal of Sea Research* 158,
1204 101871. URL: [https://www.sciencedirect.com/science/article/](https://www.sciencedirect.com/science/article/pii/S1385110119302485)
1205 [pii/S1385110119302485](https://www.sciencedirect.com/science/article/pii/S1385110119302485), doi:[https://doi.org/10.1016/j.seares.](https://doi.org/10.1016/j.seares.2020.101871)
1206 [2020.101871](https://doi.org/10.1016/j.seares.2020.101871).
- 1207 Queiroz, N., Humphries, N.E., Couto, A., Vedor, M., Da Costa, I., Sequeira, A.M., Mu-
1208 cientes, G., Santos, A.M., Abascal, F.J., Abercrombie, D.L., et al., 2021. Reply to:
1209 Caution over the use of ecological big data for conservation. *Nature* 595, E20–E28.
- 1210 Ravdas, M., Zacharioudaki, A., Korres, G., 2018. Implementation and validation of a
1211 new operational wave forecasting system of the mediterranean monitoring and forecast-

ing centre in the framework of the copernicus marine environment monitoring service.
 Natural Hazards and Earth System Sciences 18, 2675–2695.

Raybaud, V., Beaugrand, G., Dewarumez, J.M., Luczak, C., 2015. Climate-induced range
 shifts of the american jackknife clam *ensis directus* in europe. Biological Invasions 17,
 725–741.

Ready, J., Kaschner, K., South, A.B., Eastwood, P.D., Rees, T., Rius, J., Agbayani, E.,
 Kullander, S., Froese, R., 2010. Predicting the distributions of marine organisms at the
 global scale. Ecological Modelling 221, 467–478.

Rees, T., 2008. 18.9. using aquamaps for biodiversity assessment, including a prototype
 mpa (marine protected area) network design tool. The Proceedings of TDWG , 73.

Renner, I.W., Warton, D.I., 2013. Equivalence of maxent and poisson point process models
 for species distribution modeling in ecology. Biometrics 69, 274–281.

Reside, A.E., Critchell, K., Crayn, D.M., Goosem, M., Goosem, S., Hoskin, C.J., Sydes,
 T., Vanderduys, E.P., Pressey, R.L., 2019. Beyond the model: expert knowledge im-
 proves predictions of species’ fates under climate change. Ecological Applications 29,
 e01824.

Reyes, K., 2015. AquaMaps: Algorithm and Data Sources for Aquatic Organ-
 isms. [https://pacific-data.sprep.org/system/files/AquaMaps_](https://pacific-data.sprep.org/system/files/AquaMaps_Algorithm_and_Data_Sources.pdf)
[Algorithm_and_Data_Sources.pdf](https://pacific-data.sprep.org/system/files/AquaMaps_Algorithm_and_Data_Sources.pdf).

Roy-Dufresne, E., Saltr  , F., Cooke, B.D., Mellin, C., Mutze, G., Cox, T., Fordham, D.A.,

- 1232 2019. Modeling the distribution of a wide-ranging invasive species using the sampling
1233 efforts of expert and citizen scientists. *Ecology and Evolution* 9, 11053–11063.
- 1234 Russo, E., Monti, M.A., Mangano, M.C., Raffaeta, A., Sara, G., Silvestri, C., Pranovi, F.,
1235 2020. Temporal and spatial patterns of trawl fishing activities in the adriatic sea (central
1236 mediterranean sea, gsa17). *Ocean & Coastal Management* 192, 105231.
- 1237 Sabates, A., Zaragoza, N., Raya, V., 2015. Distribution and feeding dynamics of larval
1238 red mullet (*Mullus barbatus*) in the NW Mediterranean: the important role of cladocera.
1239 *Journal of Plankton Research* 37, 820–833. URL: [https://doi.org/10.1093/](https://doi.org/10.1093/plankt/fbv040)
1240 [plankt/fbv040](https://doi.org/10.1093/plankt/fbv040), doi:10.1093/plankt/fbv040.
- 1241 Sánchez-Tapia, A., de Siqueira, M.F., Lima, R.O., Barros, F.S.M., Gall, G.M., Gadelha,
1242 L.M., da Silva, L.A.E., Osthoff, C., 2017. Model-r: a framework for scalable and repro-
1243 ducible ecological niche modeling, in: *Latin American High Performance Computing*
1244 *Conference*, Springer. pp. 218–232.
- 1245 Santos, A.M.P., Ré, P., Dos Santos, A., Peliz, Á., 2006. Vertical distribution of the euro-
1246 pean sardine (*sardina pilchardus*) larvae and its implications for their survival. *Journal*
1247 *of Plankton Research* 28, 523–532.
- 1248 Sbrana, M., Zupa, W., Ligas, A., Capezzuto, F., Chatzispyrou, A., Follesa, M.C., Ganci-
1249 tano, V., Guijarro, B., Isajlovic, I., Jadaud, A., et al., 2019. Spatiotemporal abun-
1250 dance pattern of deep-water rose shrimp, *parapenaeus longirostris*, and norway lobster,
1251 *nephrops norvegicus*, in european mediterranean waters. *Scientia Marina* 83, 71–80.

- 1252 Scarponi, P., Coro, G., Pagano, P., 2018. A collection of aquamaps native layers in netcdf
1253 format. Data in brief 17, 292–296.
- 1254 Schaap, D.M., Lowry, R.K., 2010. Seadatanet–pan-european infrastructure for marine and
1255 ocean data management: unified access to distributed data sets. International Journal of
1256 Digital Earth 3, 50–69.
- 1257 Schnase, J.L., Carroll, M.L., Gill, R.L., Tamkin, G.S., Li, J., Strong, S.L., Maxwell, T.P.,
1258 Aronne, M.E., Spradlin, C.S., 2021. Toward a monte carlo approach to selecting climate
1259 variables in maxent. PloS one 16, e0237208.
- 1260 Schulzweida, U., 2020. CDO User Guide. [https://code.mpimet.mpg.de/
1261 projects/cdo/embedded/index.html#x1-5710002.12.6](https://code.mpimet.mpg.de/projects/cdo/embedded/index.html#x1-5710002.12.6).
- 1262 Shehhi, M.R.A., Samad, Y.A., 2021. Effects of the covid-19 pandemic on the oceans.
1263 Remote Sensing Letters 12, 325–334. doi:10.1080/2150704X.2021.1880658.
- 1264 Sinovčić, G., 2001. Biotic and abiotic factors influencing sardine, *sardina pilchardus*
1265 (walb.) abundance in the croatian part of the eastern adriatic. FAO Adriamed paper
1266 .
- 1267 Sion, L., Zupa, W., Calculli, C., Garofalo, G., Hidalgo, M., Jadaud, A., Lefkaditou, E.,
1268 Ligas, A., Peristeraki, P., Bitetto, I., et al., 2019. Spatial distribution pattern of european
1269 hake, *merluccius merluccius* (pisces: Merlucciidae), in the mediterranean sea. Scientia
1270 Marina 83, 21–32.
- 1271 de Siqueira, M.F., Durigan, G., de Marco Júnior, P., Peterson, A.T., 2009. Something from

1272 nothing: using landscape similarity and ecological niche modeling to find rare plant
 1273 species. *Journal for Nature Conservation* 17, 25–32.

1274 Snapshot-CNR, 2020. Synoptic Assessment of Human Pressures on Key Mediterranean
 1275 Hot Spots: The Snapshot-CNR project. <http://snapshot.cnr.it>.

1276 Tanhua, T., Pouliquen, S., Hausman, J., O'Brien, K., Bricher, P., De Bruin, T., Buck, J.J.,
 1277 Burger, E.F., Carval, T., Casey, K.S., et al., 2019. Ocean fair data services. *Frontiers in*
 1278 *Marine Science* 6, 440.

1279 Theil, H., 1982. Some recent and new results on the maximum entropy distribution. *Statis-*
 1280 *tics & Probability Letters* 1, 17–22.

1281 Toonen, H.M., Bush, S.R., 2020. The digital frontiers of fisheries governance: Fish at-
 1282 traction devices, drones and satellites. *Journal of environmental policy & planning* 22,
 1283 125–137.

1284 Trifonova, N., Maxwell, D., Pinnegar, J., Kenny, A., Tucker, A., 2017. Predicting ecosys-
 1285 tem responses to changes in fisheries catch, temperature, and primary productivity with
 1286 a dynamic bayesian network model. *ICES Journal of Marine Science* 74, 1334–1343.

1287 Troupin, C., Barth, A., Sirjacobs, D., Ouberdous, M., Brankart, J.M., Brasseur, P., Rixen,
 1288 M., Alvera-Azcárate, A., Belounis, M., Capet, A., et al., 2012. Generation of analysis
 1289 and consistent error fields using the data interpolating variational analysis (diva). *Ocean*
 1290 *Modelling* 52, 90–101.

1291 Troupin, C., Machin, F., Ouberdous, M., Sirjacobs, D., Barth, A., Beckers, J.M., 2010.

1292 High-resolution climatology of the northeast atlantic using data-interpolating variational
 1293 analysis (diva). *Journal of Geophysical Research: Oceans* 115.

1294 Ungaro, N., Gramolini, R., 2006. Possible effect of bottom temperature on distribution
 1295 of *parapenaeus longirostris* (lucas, 1846) in the southern adriatic (mediterranean sea).
 1296 *Turkish Journal of Fisheries and Aquatic Sciences* 6, –.

1297 United Nations, 2021a. Cooling La Niña is on the wane, but temperatures set to rise: UN
 1298 weather agency. <https://news.un.org/en/story/2021/02/1084222>.

1299 United Nations, 2021b. UN Decade on Ecosystem Restoration. [https://www.](https://www.decadeonrestoration.org/)
 1300 [decadeonrestoration.org/](https://www.decadeonrestoration.org/).

1301 Von Schuckmann, K., Le Traon, P.Y., Smith, N., Pascual, A., Brasseur, P., Fennel, K.,
 1302 Djavidnia, S., Aaboe, S., Fanjul, E.A., Autret, E., et al., 2018. Copernicus marine
 1303 service ocean state report. *Journal of Operational Oceanography* 11, S1–S142.

1304 Wang, L., Kerr, L.A., Record, N.R., Bridger, E., Tupper, B., Mills, K.E., Armstrong, E.M.,
 1305 Pershing, A.J., 2018. Modeling marine pelagic fish species spatiotemporal distributions
 1306 utilizing a maximum entropy approach. *Fisheries Oceanography* 27, 571–586.

1307 Warren, D.L., Seifert, S.N., 2011. Ecological niche modeling in maxent: the importance
 1308 of model complexity and the performance of model selection criteria. *Ecological appli-*
 1309 *cations* 21, 335–342.

1310 Watelet, S., Back, Ö., Barth, A., Beckers, J.M., 2016. Data-interpolating variational anal-
 1311 ysis (diva) software: recent development and application, in: *Proceedings of the EGU*
 1312 *General Assembly 2016, European Geosciences Union General Assembly*. p. 1.

- 1313 Weatherdon, L.V., Magnan, A.K., Rogers, A.D., Sumaila, U.R., Cheung, W.W., 2016.
1314 Observed and projected impacts of climate change on marine fisheries, aquaculture,
1315 coastal tourism, and human health: an update. *Frontiers in Marine Science* , 48.
- 1316 Weber, M.M., Stevens, R.D., Diniz-Filho, J.A.F., Grelle, C.E.V., 2017. Is there a corre-
1317 lation between abundance and environmental suitability derived from ecological niche
1318 modelling? a meta-analysis. *Ecography* 40, 817–828.
- 1319 Werdell, P.J., Bailey, S.W., 2005. An improved in-situ bio-optical data set for ocean color
1320 algorithm development and satellite data product validation. *Remote sensing of envi-*
1321 *ronment* 98, 122–140.
- 1322 Wernberg, T., Bennett, S., Babcock, R.C., De Bettignies, T., Cure, K., Depczynski, M.,
1323 Dufois, F., Fromont, J., Fulton, C.J., Hovey, R.K., et al., 2016. Climate-driven regime
1324 shift of a temperate marine ecosystem. *Science* 353, 169–172.
- 1325 World Meteorological Organization, 2021. Climate change indicators and impacts wors-
1326 ened in 2020. [https://public.wmo.int/en/media/press-release/](https://public.wmo.int/en/media/press-release/climate-change-indicators-and-impacts-worsened-2020)
1327 [climate-change-indicators-and-impacts-worsened-2020](https://public.wmo.int/en/media/press-release/climate-change-indicators-and-impacts-worsened-2020).
- 1328 WWF, 2020. World Wide Fund for Nature - Impact of COVID-19 on Mediter-
1329 ranean Fisheries. [https://www.wwfmmi.org/what_we_do/fisheries/](https://www.wwfmmi.org/what_we_do/fisheries/transforming_small_scale_fisheries/impact_of_covid_on_mediterranean_fisheries/)
1330 [transforming_small_scale_fisheries/impact_of_covid_on_](https://www.wwfmmi.org/what_we_do/fisheries/transforming_small_scale_fisheries/impact_of_covid_on_mediterranean_fisheries/)
1331 [mediterranean_fisheries/](https://www.wwfmmi.org/what_we_do/fisheries/transforming_small_scale_fisheries/impact_of_covid_on_mediterranean_fisheries/).
- 1332 Yunus, A.P., Masago, Y., Hijioka, Y., 2020. Covid-19 and surface water quality: Improved
1333 lake water quality during the lockdown. *Science of the Total Environment* 731, 139012.

- 1334 Zaniewski, A.E., Lehmann, A., Overton, J.M., 2002. Predicting species spatial distribu-
1335 tions using presence-only data: a case study of native new zealand ferns. *Ecological*
1336 *modelling* 157, 261–280.
- 1337 Zavatarelli, M., Raicich, F., Bregant, D., Russo, A., Artegiani, A., 1998. Cli-
1338 matological biogeochemical characteristics of the adriatic sea. *Journal of*
1339 *Marine Systems* 18, 227–263. URL: [https://www.sciencedirect.](https://www.sciencedirect.com/science/article/pii/S0924796398000141)
1340 [com/science/article/pii/S0924796398000141](https://www.sciencedirect.com/science/article/pii/S0924796398000141), doi:[https:](https://doi.org/10.1016/S0924-7963(98)00014-1)
1341 [//doi.org/10.1016/S0924-7963\(98\)00014-1](https://doi.org/10.1016/S0924-7963(98)00014-1).
- 1342 Zeng, Y., Low, B.W., Yeo, D.C., 2016. Novel methods to select environmental variables
1343 in maxent: A case study using invasive crayfish. *Ecological Modelling* 341, 5–13.
- 1344 Zhang, G., Zhu, A.X., Windels, S.K., Qin, C.Z., 2018. Modelling species habitat suitabil-
1345 ity from presence-only data using kernel density estimation. *Ecological Indicators* 93,
1346 387–396.

Table 1: Discrepancy between the ecological niche models of the eight species involved in our experiment. Model names refer to floating sensor models for 2015-2018 (FS 2015-2018), 2019 (FS 2019), 2020 (FS 2020), and AquaMaps 2019 and 2050. Coloured numbers refer to Cohen’s kappa values corresponding to at-least-moderate (green), slight (orange), or poor agreement (red) according to Landis & Koch interpretation. Bold-highlighted text indicates the most similar distribution for each model. Coloured species names indicate habitat gain (green), change (red), or stability (blue) in 2020 with respect to 2015-2018.

Sepia officinalis						
	FS 2015-2018	FS 2019	FS 2020	AquaMaps 2019	AquaMaps 2050	
FS 2015-2018	-	10.06%	12.36%	15.24%	21.71%	
FS 2019	10.06%	-	7.18%	15.50%	22.71%	
FS 2020	12.36%	7.18%	-	14.87%	24.72%	
AquaMaps 2019	15.24%	15.50%	14.87%	-	43.14%	
AquaMaps 2050	21.71%	22.71%	24.72%	43.14%	-	
Merluccius merluccius						
	FS 2015-2018	FS 2019	FS 2020	AquaMaps 2019	AquaMaps 2050	
FS 2015-2018	-	18.53%	17.82%	25.92%	34.25%	
FS 2019	18.53%	-	5.89%	22.61%	40.90%	
FS 2020	17.82%	5.89%	-	22.47%	41.03%	
AquaMaps 2019	25.92%	22.61%	22.47%	-	52.26%	
AquaMaps 2050	34.25%	40.90%	41.03%	52.26%	-	
Mullus barbatus						
	FS 2015-2018	FS 2019	FS 2020	AquaMaps 2019	AquaMaps 2050	
FS 2015-2018	-	18.53%	16.24%	22.61%	24.28%	
FS 2019	18.53%	-	9.20%	18.88%	30.43%	
FS 2020	16.24%	9.20%	-	19.60%	27.42%	
AquaMaps 2019	22.61%	18.88%	19.60%	-	38.25%	
AquaMaps 2050	24.28%	30.43%	27.42%	38.25%	-	
Sardina pilchardus						
	FS 2015-2018	FS 2019	FS 2020	AquaMaps 2019	AquaMaps 2050	
FS 2015-2018	-	14.51%	22.84%	16.69%	21.64%	
FS 2019	14.51%	-	29.60%	24.22%	29.17%	
FS 2020	22.84%	29.60%	-	18.32%	20.89%	
AquaMaps 2019	16.69%	24.22%	18.32%	-	32.69%	
AquaMaps 2050	21.64%	29.17%	20.89%	32.69%	-	
Parapenaeus longirostris						
	FS 2015-2018	FS 2019	FS 2020	AquaMaps 2019	AquaMaps 2050	
FS 2015-2018	-	47.13%	34.34%	21.71%	26.35%	
FS 2019	47.13%	-	20.83%	21.83%	58.85%	
FS 2020	34.34%	20.83%	-	20.70%	41.91%	
AquaMaps 2019	21.71%	21.83%	20.70%	-	47.88%	
AquaMaps 2050	26.35%	58.85%	41.91%	47.88%	-	
Solea solea						
	FS 2015-2018	FS 2019	FS 2020	AquaMaps 2019	AquaMaps 2050	
FS 2015-2018	-	6.18%	6.75%	11.23%	34.63%	
FS 2019	6.18%	-	2.73%	11.23%	34.63%	
FS 2020	6.75%	2.73%	-	10.85%	34.63%	
AquaMaps 2019	11.23%	11.23%	10.85%	-	52.46%	
AquaMaps 2050	34.63%	34.63%	34.63%	52.46%	-	
Squilla mantis						
	FS 2015-2018	FS 2019	FS 2020	AquaMaps 2019	AquaMaps 2050	
FS 2015-2018	-	12.07%	4.74%	19.70%	19.20%	
FS 2019	12.07%	-	10.63%	19.70%	17.57%	
FS 2020	4.74%	10.63%	-	19.70%	19.07%	
AquaMaps 2019	19.70%	19.70%	19.70%	-	41.87%	
AquaMaps 2050	19.20%	17.57%	19.07%	41.87%	-	
Engraulis encrasicolus						
	FS 2015-2018	FS 2019	FS 2020	AquaMaps 2019	AquaMaps 2050	
FS 2015-2018	-	12.79%	12.07%	21.90%	30.80%	
FS 2019	12.79%	-	4.45%	21.90%	30.80%	
FS 2020	12.07%	4.45%	-	21.90%	30.65%	
AquaMaps 2019	21.90%	21.90%	21.90%	-	53.00%	
AquaMaps 2050	30.80%	30.80%	30.65%	53.00%	-	

Table 2: Suitability score comparison between the ecological niche models of the eight species involved in our experiment. Model names indicate floating sensor models for 2015-2018 (FS 2015-2018), 2019 (FS 2019), 2020 (FS 2020), and AquaMaps 2019 and 2050. Scores are reported only for the FS models to ease the reading. Coloured numbers highlight habitat gain (green), loss (red), or stability (blue) in 2020. Coloured species names indicate habitat gain (green), change (red), or stability (blue) in 2020 with respect to 2015-2018.

<i>Sepia officinalis</i>					
	FS 2015-2018	FS 2019	FS 2020	AquaMaps 2019	AquaMaps 2050
FS 2015-2018	-	Loss (-0.29%)	Loss (-3.95%)	Loss	Gain
FS 2019	Gain (+0.29%)	-	Loss (-0.14%)	Loss	Gain
FS 2020	Gain (+3.95%)	Gain (+0.14%)	-	Loss	Gain
AquaMaps 2019	Gain	Gain	Gain	-	Gain
AquaMaps 2050	Loss	Loss	Loss	Loss	-
<i>Merluccius merluccius</i>					
	FS 2015-2018	FS 2019	FS 2020	AquaMaps 2019	AquaMaps 2050
FS 2015-2018	-	Loss (-7.04%)	Loss (-5.68%)	Loss	Gain
FS 2019	Gain (+7.04%)	-	Gain (+0.36%)	Loss	Gain
FS 2020	Gain (+5.68%)	Loss (-0.36%)	-	Loss	Gain
AquaMaps 2019	Gain	Gain	Gain	-	Stable
AquaMaps 2050	Loss	Loss	Loss	Stable	-
<i>Mullus barbatus</i>					
	FS 2015-2018	FS 2019	FS 2020	AquaMaps 2019	AquaMaps 2050
FS 2015-2018	-	Loss (-7.61%)	Loss (-3.38%)	Loss	Gain
FS 2019	Gain (+7.61%)	-	Gain (+1.94%)	Loss	Gain
FS 2020	Gain (+3.38%)	Loss (-1.94%)	-	Loss	Gain
AquaMaps 2019	Gain	Gain	Gain	-	Gain
AquaMaps 2050	Loss	Loss	Loss	Loss	-
<i>Sardina pilchardus</i>					
	FS 2015-2018	FS 2019	FS 2020	AquaMaps 2019	AquaMaps 2050
FS 2015-2018	-	Loss (-4.31%)	Loss (-4.6%)	Loss	Gain
FS 2019	Gain (+4.31%)	-	Gain (+5.46%)	Gain	Gain
FS 2020	Gain (+4.6%)	Loss (-5.46%)	-	Gain	Gain
AquaMaps 2019	Gain	Loss	Loss	-	Gain
AquaMaps 2050	Loss	Loss	Loss	Loss	-
<i>Parapenaeus longirostris</i>					
	FS 2015-2018	FS 2019	FS 2020	AquaMaps 2019	AquaMaps 2050
FS 2015-2018	-	Loss (-14.87%)	Loss (-8.33%)	Loss	Gain
FS 2019	Gain (+14.87%)	-	Gain (+7.04%)	Loss	Gain
FS 2020	Gain (+8.33%)	Loss (-7.04%)	-	Loss	Gain
AquaMaps 2019	Gain	Gain	Gain	-	Gain
AquaMaps 2050	Loss	Loss	Loss	Loss	-
<i>Solea solea</i>					
	FS 2015-2018	FS 2019	FS 2020	AquaMaps 2019	AquaMaps 2050
FS 2015-2018	-	Stable	Loss (-0.5%)	Gain	Gain
FS 2019	Stable	-	Stable	Gain	Gain
FS 2020	Gain (+0.5%)	Stable	-	Gain	Gain
AquaMaps 2019	Loss	Loss	Loss	-	Gain
AquaMaps 2050	Loss	Loss	Loss	Loss	-
<i>Squilla mantis</i>					
	FS 2015-2018	FS 2019	FS 2020	AquaMaps 2019	AquaMaps 2050
FS 2015-2018	-	Loss (-1.22%)	Loss (-0.36%)	Loss	Gain
FS 2019	Gain (+1.22%)	-	Gain (+0.72%)	Loss	Gain
FS 2020	Gain (+0.36%)	Loss (-0.72%)	-	Loss	Gain
AquaMaps 2019	Gain	Gain	Gain	-	Gain
AquaMaps 2050	Loss	Loss	Loss	Loss	-
<i>Engraulis encrasicolus</i>					
	FS 2015-2018	FS 2019	FS 2020	AquaMaps 2019	AquaMaps 2050
FS 2015-2018	-	Loss (-5.6%)	Stable	Gain	Gain
FS 2019	Gain (+5.6%)	-	Gain (+1.15%)	Stable	Gain
FS 2020	Stable	Loss (-1.15%)	-	Gain	Gain
AquaMaps 2019	Loss	Stable	Loss	-	Stable
AquaMaps 2050	Loss	Loss	Loss	Stable	-

Table 3: Median, 1st and 3rd quartiles of the environmental parameter distributions used in our experiment over the Adriatic Sea, estimated from Argo data. *Average* aggregation type indicates parameter average over the entire water column.

Parameter name	Aggregation type	Years	Median	1st Quartile	3rd Quartile
Temperature (° C)	average	2015-2018	14.95	14.94	15.02
		2019	14.74	14.74	14.75
		2020	15.26	15.25	15.26
	bottom	2015-2018	14.15	14.14	14.16
		2019	14.10	14.09	14.10
		2020	14.32	14.31	14.32
	surface	2015-2018	16.58	16.50	18.48
		2019	19.67	18.51	19.71
		2020	18.40	18.35	18.55
Salinity (PSU)	average	2015-2018	38.83	38.83	38.83
		2019	38.90	38.90	38.90
		2020	38.97	38.97	38.97
	bottom	2015-2018	38.82	38.82	38.82
		2019	38.86	38.85	38.86
		2020	38.90	38.89	38.90
	surface	2015-2018	38.78	38.77	38.78
		2019	38.80	38.80	38.82
		2020	39.01	39.00	39.01
Chlorophyll-a (mg/m^3)	average	2015-2018	0.0391	0.0389	0.0392
		2019	0.0366	0.0365	0.0377
		2020	0.0343	0.0331	0.0344
	bottom	2015-2018	0.0051	0.0027	0.0052
		2019	0.0056	0.0056	0.0057
		2020	0.0028	0.0027	0.0029
	surface	2015-2018	0.0436	0.0432	0.0438
		2019	0.2213	0.2202	0.2222
		2020	0.1896	0.1888	0.1907
Dissolved oxygen ($\mu mol/kg$)	average	2015-2018	234.12	228.72	234.26
		2019	220.50	219.88	220.53
		2020	213.70	213.67	213.72
	bottom	2015-2018	214.32	212.41	214.39
		2019	216.81	216.40	216.84
		2020	210.33	210.16	210.35
	surface	2015-2018	228.36	228.25	228.64
		2019	227.80	227.66	227.92
		2020	214.73	214.47	214.84

Table 4: Percent contribution and permutation importance of the most habitat-predictive parameters for the 8 analysed species. Bold-highlighted text indicates, for each species, the major drivers of habitat change from 2015-2018 to 2020. Coloured species names indicate habitat gain (green), change (red), or stability (blue) in 2020 with respect to 2015-2018.

Species name	Parameter	Percent contribution (%)	Permutation importance (%)
Sepia officinalis	depth	77.6	59.3
	average dissolved oxygen	5.4	8.4
	average salinity	5.3	21.2
	bottom dissolved oxygen	4.9	0
	bottom temperature	4.6	0.1
	bottom salinity	1.4	5.6
	surface chlorophyll-a	0.8	5.5
Merluccius merluccius	bottom temperature	48.2	27.6
	average chlorophyll-a	24.6	14.2
	depth	7.8	26.4
	surface chlorophyll-a	6.4	16.5
	average salinity	4.7	5.4
	surface dissolved oxygen	3.9	3
	surface salinity	2.4	1.5
	average temperature	1.9	5.4
Mullus barbatus	bottom temperature	49.5	24.7
	average chlorophyll-a	24.7	13.6
	surface dissolved oxygen	6.7	6.8
	depth	6.5	20.1
	bottom chlorophyll-a	5.5	17.4
	surface chlorophyll-a	3.1	10.4
	bottom dissolved oxygen	2.3	3.8
	surface salinity	1.7	3.2
Sardina pilchardus	bottom chlorophyll-a	66.6	54.4
	average dissolved oxygen	16.7	0.5
	average chlorophyll-a	11.9	20
	bottom dissolved oxygen	4.2	0
	depth	0.6	25.1
Parapenaeus longirostris	depth	66.2	45
	surface temperature	12.9	40.4
	average temperature	9.6	14.5
	average dissolved oxygen	8.1	0
	surface dissolved oxygen	3.2	0.1
Solea solea	depth	80.6	84.9
	average temperature	9.7	0
	average dissolved oxygen	5.1	0
	bottom chlorophyll-a	2.8	9.7
	average salinity	1.8	5.4
Squilla mantis	depth	66	77.3
	bottom chlorophyll-a	14.4	6.3
	average temperature	14.1	16.1
	surface temperature	4.1	0.3
	bottom salinity	1.5	0
Engraulis encrasicolus	depth	63	31
	surface dissolved oxygen	20.1	43.6
	bottom chlorophyll-a	5.6	25.4
	bottom dissolved oxygen	5.5	0
	average chlorophyll-a	3.5	0
	average dissolved oxygen	2.4	0

Table 5: Summary of the principal environmental parameters that drove species distribution change in 2020. For each parameter, the table reports (i) the general (increasing/decreasing) trend with respect to the past years, (ii) the main reasons of the change, (iii-iv) the species whose distributions were positively affected (i.e. they increased in 2020) or negatively affected by that parameter change.

Principal parameters that drove selected-species distribution change in 2020	General trend in 2020 wrt past years	Possible reason of the change	Species with positively affected distribution by the change	Species with negatively affected distribution by the change
Temperature	Increasing	Climate change	<i>Sepia officinalis</i> , <i>Merluccius merluccius</i> , <i>Mullus barbatus</i>	<i>Parapenaeus longirostris</i>
Dissolved Oxygen	Decreasing	Climate change and pollution	<i>Sepia officinalis</i>	<i>Sardina pilchardus</i> , <i>Parapenaeus longirostris</i>
Chlorophyll-a	Decreasing	COVID-19 pandemic	<i>Merluccius merluccius</i> , <i>Mullus barbatus</i>	<i>Sardina pilchardus</i>

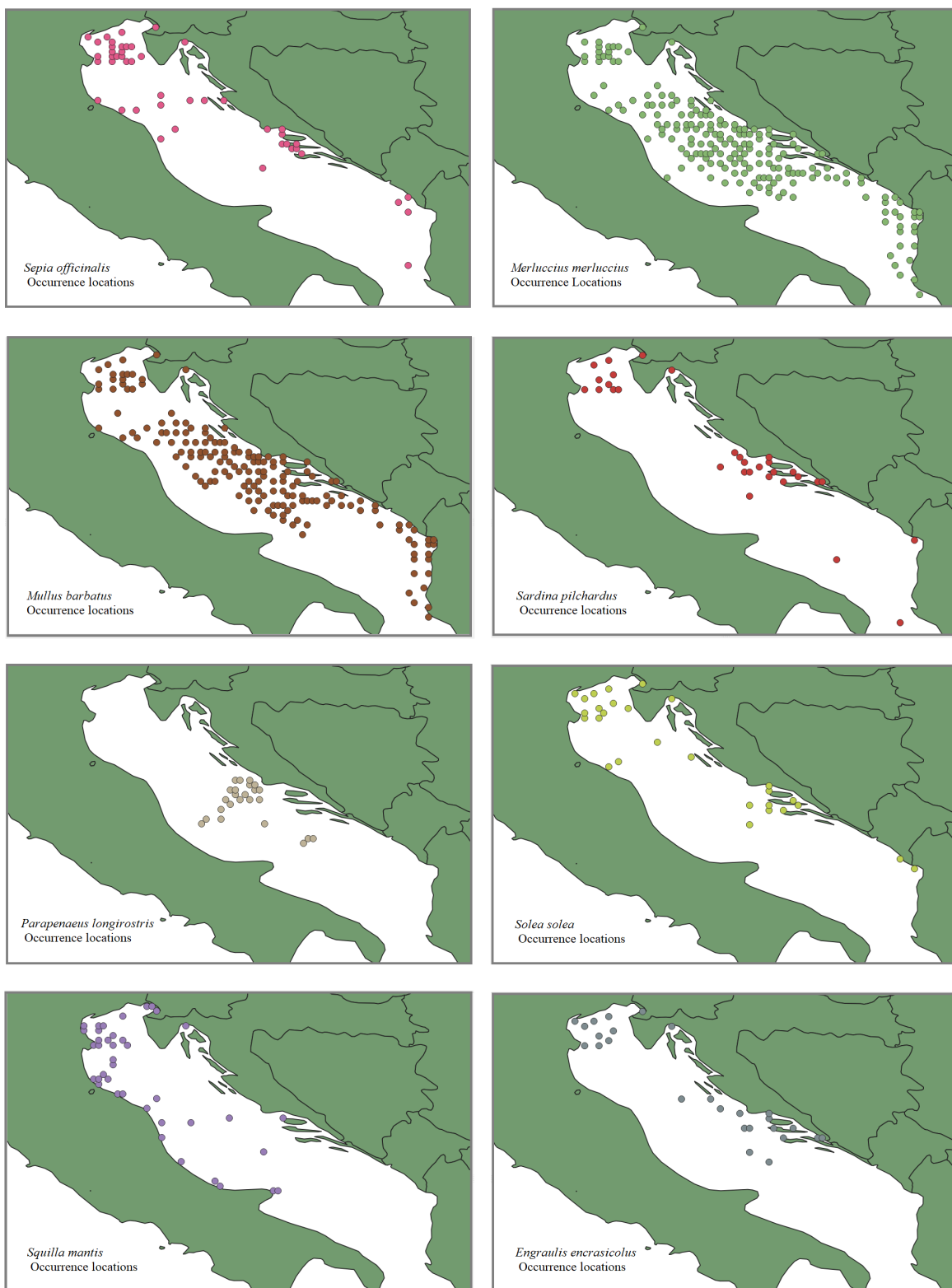


Figure 1: Distribution of the analysed species' occurrence records, used for our floating sensor based ecological niche models.

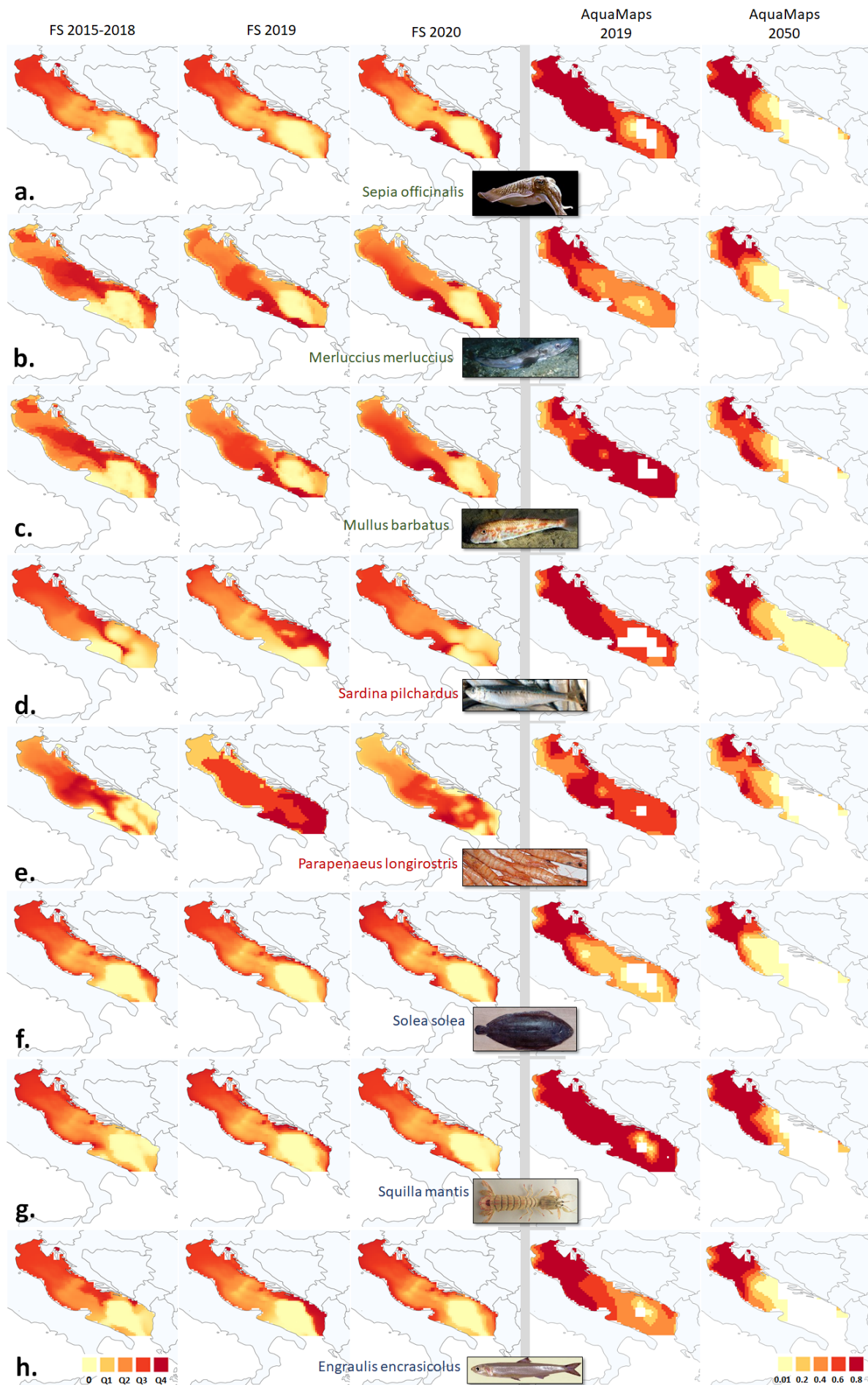


Figure 2: Ecological niches estimated by our floating sensor based (FS) models for 2015-2018, 2019, and 2020, and AquaMaps 2019 and 2050 over the eight analysed species. Coloured species names indicate habitat gain (green), change (red), or stability (blue) in 2020 with respect to 2015-2018.

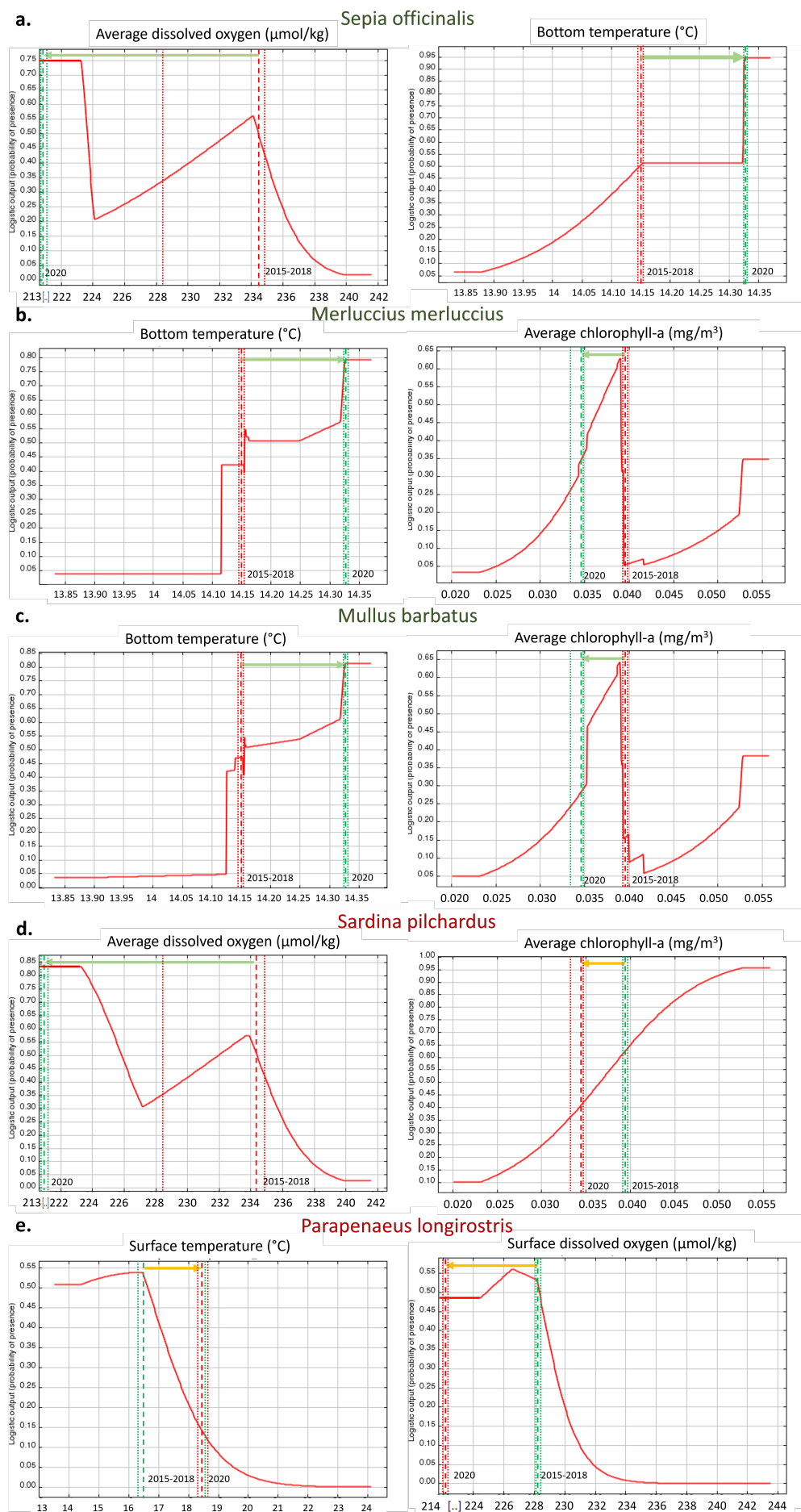


Figure 3: Single-parameter MaxEnt probability densities across the studied species. Only the charts of the key parameters driving habitat gain and change are reported. Coloured species names in the chart titles indicate those that gained (green) or changed (red) habitat in 2020 with respect to 2015-2018. Vertical bars highlight the values in 2015-2018 and 2020 at the intersection with medians as dashed lines and quartiles 1 and 3 as dotted lines. A green horizontal arrow, from a red to a green vertical line, indicates a general habitat suitability increase from 2015-2018 to 2020. Conversely, a yellow horizontal arrow, from a green to a red vertical line, indicates habitat suitability decrease from 2015-2018 to 2020.